Cerebral correlates of impaired grating perception in individual, psychophysically assessed human amblyopes

Lars Muckli [a,b], Stefan Kieß [a], Nathalie Tonhausen [a], Wolf Singer [a,b], Rainer Goebel [a,c], Ruxandra Sireteanu [a,d,e,*]

[a] *Department of Neurophysiology, Max Planck Institute for Brain Research, Deutschordenstrasse 46, 60528 Frankfurt a. M., Germany*
[b] *Brain Imaging Center Frankfurt, Schleusenweg 2-6, 60590 Frankfurt, Germany*
[c] *Department of Neurocognition, Faculty of Psychology, Maastricht University, Maastricht, The Netherlands*
[d] *Department of Biological Psychology, Institute for Psychology, Johann Wolfgang Goethe-University, Mertonstrasse 17, 60054 Frankfurt, Germany*
[e] *Department of Biomedical Engineering, College of Engineering, Boston University, Cumming Street, Boston, MA, USA*

Abstract

We investigated neuronal correlates of amblyopic deficits resulting from early onset strabismus or anisometropia by monitoring individual responses in retinotopically mapped cortical visual areas with functional magnetic resonance imaging (fMRI) in eight psychophysically assessed adult amblyopes. In lower visual areas (V1/V2), grating stimuli presented to the normal and the amblyopic eye evoked strong cortical responses, while responses to the amblyopic eye were progressively reduced in higher areas on the central visual pathway (V3a/VP; V4/V8; lateral occipital complex, LOC). Selective reduction for high spatial frequency gratings was especially obvious in LOC. This suggests that transmission of activity from the amblyopic eye is increasingly impaired while it is relayed towards higher processing levels. Elevated responses in parts of areas V1 and V2 to monocular stimulation of the amblyopic eye might be related to the spatial and temporal distortions experienced by some amblyopic subjects.
© 2005 Elsevier Ltd. All rights reserved.

Keywords: Amblyopia; Functional magnetic resonance imaging; Retinotopic mapping; Extrastriate visual cortex; Perceptual distortion

1. Introduction

Amblyopia is a developmental deficit caused by inadequate visual stimulation early in life. It is defined clinically by a reduction of visual acuity in otherwise healthy and properly corrected eyes. The most common factors leading to amblyopia are a misalignment of the visual axes of the two eyes (strabismus), unequal refractive power in the two eyes (anisometropia), or a physical obstruction, like a lens opacity (cataract) or a drooping eyelid (ptosis), preventing visual signals from reaching the retina of one or both eyes (visual deprivation). Strabismic subjects use only one eye at a time for vision in order to avoid double images. If, rather than alternating between the two eyes, they use always the same eye, the other develops amblyopia, presumably because the cortical networks connected to this suppressed eye do not develop normally. Subjects report reduced visual acuity and difficulties with figure-ground segregation when viewing with the amblyopic eye.

It has been suggested that strabismic and anisometropic amblyopia form two separate syndromes, possibly involving different neural substrates: while anisometropic amblyopia is believed to be a mild form of visual deprivation, strabismic amblyopia was proposed to result from active suppression of the deviating eye. The different aetiologies can lead to different deficits: in anisometropic and deprivation amblyopia, reduced acuity is the dominant disturbance. With strabismic amblyopia, there may be additional symptoms such as anomalous retinal correspondence, disturbed eye–hand coordination, and different patterns of

---

* Corresponding author. Tel.: +49 69 96769277; fax: +49 69 96769740.
  E-mail addresses: Muckli@mpih-frankfurt.mpg.de (L. Muckli), Sireteanu@mpih-frankfurt.mpg.de (R. Sireteanu).

interocular suppression (cf. Duke-Elder, 1973; Fronius & Sireteanu, 1994; Leonards & Sireteanu, 1993; Sireteanu & Fronius, 1981, 1989; von Noorden, 1980; Yu & Levi, 1998). Strabismic amblyopes experience difficulties to separate nearby visual contours (crowding: Hess, Dakin, & Kapoor, 2000; Hess, Dakin, Tewfik, & Brown, 2001; Levi & Klein, 1983, 1985), they show deficits in spatial localization (Bedell & Flom, 1981, 1983; Levi & Klein, 1985) and exhibit spatial uncertainty (Bedell & Flom, 1981, 1983; Demanins & Hess, 1996; Fronius & Sireteanu, 1989; Wang, Levi, & Klein, 1998). Perceptual distortions were described in strabismic, but not in anisometropic amblyopes (Barrett, Pacey, Bradley, Thibos, & Morill, 2003; Bradley & Freeman, 1985; Hess, Campbell, & Greenhalgh, 1978; Lagrèze & Sireteanu, 1991; Pugh, 1958; Sireteanu, Lagrèze, & Constantinescu, 1993). Strabismic amblyopes experience temporal instability, in addition to spatial distortions, when using their amblyopic eye (Barrett et al., 2003; Sireteanu, 2000a).

Physiological studies in cats rendered amblyopic by inducing an early deprivation or a surgical strabismus support the suggestion of a functional dichotomy between strabismic and deprivation amblyopia: Visually deprived cats show a reduction in the relative frequency of single cells driven by the affected eye already in area 17 (cf. Wiesel, 1982; Wiesel & Hubel, 1963). In strabismic kittens with a demonstrated loss of function, the frequency of cells driven by the amblyopic eye is only mildly reduced in area 17 (cf. Chino, Shansky, Jankowski, & Banser, 1983; Roelfsema, König, Engel, Sireteanu, & Singer, 1994; Singer, von Grünau, & Rauschecker, 1980). A substantial loss of cells driven by the affected eye occurs in extrastriate visual areas such as the lateral suprasylvian areas PMLS and PLLS (Sireteanu & Best, 1992) and area 21a (Schröder, Fries, Roelfsema, Singer, & Engel, 2002). The hypothesis was put forward that strabismic amblyopia might be associated with a selective loss of response synchronization at high spatial frequencies among otherwise well responding striate cortex cells driven by the amblyopic eye (Roelfsema et al., 1994). This lack of temporal structure between members of active cell assemblies in primary visual cortex has been proposed to be the cause for the reduced neuronal activity in extrastriate visual regions (Sireteanu, 2000a, 2000b).

Studies in monkeys reared with an early surgically induced strabismus or an artificial anisometropia showed a reduction of behaviorally tested contrast sensitivity and grating acuity in the affected eyes (Kiorpes, Kiper, O'Keefe, Cavanaugh, & Movshon, 1998). Both groups of animals showed a loss of binocular cells in the primary visual cortex, but only anisometropic monkeys showed a reduction in the incidence of cells driven by the amblyopic eye. In strabismically amblyopic monkeys, both eyes were equally represented in area 17, but the cells activated by the amblyopic eye had lower contrast sensitivities, optimal spatial frequencies and visual acuities; still, the physiological deficit in the primary visual cortex was smaller than the behavioural deficit. Thus, the physiological deficits in area 17 were not sufficient to explain the full range of perceptual deficits in strabismic amblyopia (Kiorpes et al., 1998; for reviews, see Kiorpes, 2002; Kiorpes & McKee, 1999).

In humans, the neural basis of amblyopia is still controversial. Studies using positron-emission tomography (PET), functional magnetic resonance imaging (fMRI) or magnetoencephalography (MEG) produced heterogeneous results, ranging from a reduction of cortical activity in primary visual areas (Algaze, Roberts, Leguire, Schmalbrock, & Rogers, 2002; Anderson, Holliday, & Harding, 1999; Demer, Grafton, Marg, Mazziotta, & Nuwer, 1997; Demer, von Noorden, Volkow, & Gould, 1988; Goodyear, Nicolle, Humphrey, & Menon, 2000; Kabasakal et al., 1995; Lee et al., 2001) to a reduction of activity in areas V2 and V3 ipsilateral to the amblyopic eye (Imamura et al., 1997).

A recent, well-controlled fMRI study showed that strabismic amblyopes have reduced activity in early visual areas including V1 (Barnes, Hess, Dumoulin, Achtman, & Pike, 2001). Using high-field fMRI, Goodyear, Nicolle, and Menon (2002) found a reduction of ocular dominance columns for the amblyopic eyes of subjects with early-onset amblyopia. A selective reduction of activity was reported in the face-related cortical area in the fusiform gyrus, but not in the building-related area in the colateral sulcus or in the striate cortex, thus suggesting that the amblyopic loss might involve some higher-order, but not the early cortical visual areas (Lerner et al., 2003).

These studies were conducted with subjects with different densities of amblyopia, using different visual stimuli and different stimulation protocols. One possible reason for the different results might be that the earlier studies did not use retinotopic mapping to separate the various visual areas. A systematic study, relating orthoptic and psychophysical data of individual subjects with the assessment of brain activity in several retinotopically identified areas in the striate, extrastriate and higher-level cortical regions of the same subjects, is still lacking. In the present study, we attempted to fill this gap. We applied fMRI to identify visual areas with a retinotopic mapping procedure and to investigate the sites of activation deficits in individual strabismic and anisometropic amblyopes that have been characterized by prior extensive and careful orthoptic and psychophysical tests. To enable a direct comparison between perceptual and cortical activation patterns of the subjects, we used gratings with different spatial frequencies in both psychophysical and brain imaging experiments. We quantified the activation patterns in retinotopic visual areas V1, V2, V3, VP, V3a, V4/V8, and LOC.

Based on the results of electrophysiological experiments, we hypothesized that activation through the amblyopic eye should be progressively reduced at increasingly higher cortical levels on the ventral stream of strabismic amblyopes. Our results confirmed this hypothesis. Similar effects were seen in anisometropic amblyopes. In addition, we found an occasional enhancement of activity through the amblyopic eye in parts of the early visual areas V1 and V2 in some amblyopic subjects.

Part of the results of this study were presented in abstract form (Kieß, Sireteanu, Goebel, Lanfermann, & Muckli, 2001; Muckli et al., 1998; Sireteanu et al., 1998).

2. Methods

2.1. Subject recruitment and orthoptic assessment

The subjects were volunteers recruited through leaflets distributed in the Frankfurt area and through clinical referrals. All subjects underwent a comprehensive orthoptic examination by a professional orthoptist, including: objective refraction, tested with a Rodenstock Refractometer; subjective refraction for near and far, tested with a Rodamat Foropter; corrected Snellen visus for near and far (single optotypes, consisting of letters, figures and Landolt *C*'s; *C* test for single optotypes after Hohman and Haase; Oculus Optikgeräte, Dutenhofen, Germany); eye motility; monocular fixation pattern; squint angle assessed with the prism and cover test; stereopsis assessed with the TNO (Lameris Instrumenten b.v., Utrecht, NL), Randot (Stereo Optical, Chicago, USA) and Titmus stereotest (Titmus Optical, Petersburg, USA); retinal correspondence assessed with the Maddox cross in connection with dark and light red glasses and the striated glasses of Bagolini. In addition, the clinical history of each subject was recorded (for details, see Sireteanu & Fronius, 1981).

The study was performed in accordance with the tenets of the Declaration of Helsinki. The experiments had been approved by the Ethical Committee of the Frankfurt University. Written informed consent was obtained from all subjects prior to the study after the purpose and procedure were fully explained.

2.2. Subjects

To be included in the experimental group, subjects were required to have an amblyopic deficit of at least two lines on a Snellen chart test. The subjects were classified as strabismic or anisometropic on the basis of their presumed aetiology. They were classified as being primarily anisometropic if they had a refractive difference between the two eyes of at least 2D spherical equivalent. Subject MM was anisometropic as well as strabismic. Since he had a relatively large anisometropia and the onset of his divergent squint was relatively late (3–4 years of age), he was included in the anisometropic group. Additional criteria for inclusion in the experiments were: no claustrophobia; no metal parts in the body; no known ocular, neurological or psychiatric abnormalities; no drug intake or other medication; normal color vision.

Out of the subjects fulfilling these criteria, four anisometropic amblyopes (two females, two males) and four strabismic amblyopes (two females, two males) were selected for this study. As far as possible, the subjects in the two groups were matched for age, gender, and depth of amblyopia. In addition, we included four normally sighted, eme-tropic subjects (three females, one male) matched for age with the experimental groups. Orthoptic details of all included subjects are shown in Table 1.

2.3. Eye separation and refractive correction

One of the basic conditions for providing proper monocular data in the imaging experiments is a perfect match of the monocular stimulation conditions and a motion-free alternation of monocular stimulation of the two eyes. In order to avoid artifacts caused by mechanically closing one eye or by collecting monocular data for the two eyes in separate sessions, we opted for an optical separation of the eyes. The subjects wore red–green filters with perfectly matched luminance transmittances, ensuring that there was absolutely no cross-talk between the eyes in both psychophysical and fMRI experiments. Special care was taken to ensure a complete extinction of the complementary color. Large (41 cm × 46.5 cm) red and green filters were ordered from Oculus Optikgeräte GmbH, Dutenhofen, Germany. From these, the filters to be worn in front of the eyes were cut and fitted in light-tight but air-permissive protection goggles. Rectangular filters cut from the same material were mounted in frames placed in front of the projectors. The same material was used for the filters in the psychophysical and the imaging experiments.

To control for individual variances in spectral sensitivity, pretests were performed with four pairs of goggles: red–green (red in front of the dominant eye), green–red (green in front of the dominant eye), red–red, and green–green. To limit vision to one eye, the filters made of the same material as the goggles were flipped in alternation in front of the computer screen, during the psychophysical experiments, or in front of the stimulation projector, during the fMRI experiments. Luminances of the filtered stimuli were measured with a photometer (LiteMate III, Kollmorgen, Burbank, USA) and balanced by use of additional neutral density filters.

To ensure that the subjects' refraction was properly corrected during both the psychophysical and the imaging experiments, custom-made spectacles with metal-free rims were ordered from a professional optician for each subject, based on the objective refraction values determined during orthoptic testing and appropriate for the testing distance. These spectacles were worn under the colored goggles in all experiments.

2.4. Psychophysics

Prior to psychophysical testing, the subjects' contrast sensitivity was tested for near and far, using the Vistech Contrast Sensitivity Function Test (VCTS 6500 charts). Testing was done monocularly and binocularly, using the subjects' best refractive correction.

The psychophysical tests were performed in separate sessions, outside of the scanner and consisted of monocular and binocular measurements of grating acuity. Measured

Table 1
Orthoptic data of all subjects participating in the experiments

Subject	Gender age	Eye (#dom.)	Refraction	Visus	Fixation	Strabismus	Stereo	Correspondence	Observations
Controls									
EB	f 67	R	+0 to 0.5/90°	1.00	Foveolar	None	20″	Normal	None
		L#	+0.25 to 0.75/90	1.00	Foveolar				
NT	f 31	R	—	1.25	Foveolar	None	20″	Normal	None
		L#	—	1.50	Foveolar				
TS	m 31	R	—	1.25	Foveolar	None	20″	Normal	None
		L#	—	1.25	Foveolar				
LC	f 19	R#	—	1.25	Foveolar	None	20″	Normal	None
		L	—	1.25	Foveolar				

Subject	Gender age	Eye (*ambl.)	Refraction	Visus	Fixation	Strabismus	Stereo	Correspondence	Observations
Anisometropes									
MAM	f 67	R*	−7.0 to 2.0/170°	0.08	Foveolar	Far: −1° + VD5°	Absent	Not testable	No surgery, no therapy, first RX 50 years
		L	+1.5 sph.	1.00	Foveolar	Near: +VD5°			Anisometropia
EM	f 42	R	+0.25 to 0.5/0°	1.4	Foveolar	None	Absent	nrc	Family history, no surgery, first RX 12 years
		L*	+3.25 to 1.25/160°	0.50	Foveolar				Anisometropia
MM	m 24	R*	+3.0 to 1.25/145°	0.60	Foveolar	Far: −12°	Absent	arc	Squint onset 3–4 years, family history, no surgery, occlusion therapy
		L	+0.75 to 1.75/0°	1.25	Foveolar	Near: 10° + VD2°		7° nasal	Anisometropia
RK	m 32	R	+3.5 sph. (CL)	1.25	Foveolar	Far: none	100″	nrc	Family history, no surgery, first RX 7 years
		L*	+6.0 sph. (CL)	0.80	Foveolar	Near: +1°			Anisometropia
Strabismics									
KG	f 25	R	−3.25 to 0.25/30°	1.25	Foveolar	Far: +12°	Absent	arc	Squint onset 2–3 years, no family history, no surgery, first RX 4 years
		L*	−3.25 sph.	0.20	7–8° nasal	Near: +15°			
KSM	f 46	R*	−0.25 sph.	0.40	3° nasal	Far: +3°	Absent	harc	Family history no surgery
		L	−0.25/120°	1.00	Foveolar	Near: +3°			Microstrabismus with identity
PZ	m 33	R	+1.75 sph.	1.00	Foveolar	Far: +10°	Absent	nharc	Family history, no surgery, occlusion therapy
		L*	+3.0 sph.	0.40	Foveolar	Near: +12°		Former harmonious	
RS	m 29	R*	+3.5 to 1.0/150°	0.30	Foveolar unstable	Far: +1°	Absent	harc	No family history, no surgery occlusion therapy 6 years
		L	+2.25 sph.	1.60	Foveolar	Near: +2°			Microstrabismus

L: left eye; R: right eye; sph: diopter spherical aberration; CL: cylindrical; nrc: normal retinal correspondence; arc: anomalous retinal correspondence; harc: harmonious anomalous retinal correspondence; f: female; m: male; the amblyopic eyes are marked with an asterisk, the dominant eyes in control subjects are marked with a cross. "Visus" refers to visual acuity for far, obtained with single Snellen optotypes (letters and figures). 1.0 corresponds to 6/6 Snellen acuity.

variables were detection threshold and response latencies. Stimuli consisted of high-contrast (86%) square-wave gratings of different spatial frequencies (0.5–36 c/deg). The choice of square-wave instead of sine-wave gratings was due to the limitation of the projector used in the scanner (the highest available spatial frequency was based on a single dark and a bright pixel). All gratings were presented through a circular aperture of 9° diameter on a computer screen at 205 cm distance. Gratings of different spatial frequencies and in two different orientations (vertical or horizontal) were presented to the subject in pseudo-random order, interleaved with blank screens. Subjects performed a two-alternative forced-choice task using one of two buttons

of the computer mouse to indicate the orientation of the grating. Half of the subjects used the index finger to indicate vertical orientation and the middle finger to indicate horizontal orientation of the grating; for the other half of the subjects, the finger coding was reversed. When no grating was visible, the subject was asked to guess. The subjects had unlimited time to complete this task. Each subject was presented with gratings of at least six different spatial frequencies, differing by one octave. The range of spatial frequencies was adjusted for each subject and each eye, such as to ensure that at least two gratings were subthreshold and two suprathreshold. About 40 measurements were made for each spatial frequency. Each subject was tested

wearing his/her prescribed spectacles for correction of refractive errors. Each subject participated in two sessions (a binocular and a monocular session). In each session, all possible combinations of goggles were used (red–green and green–red for the monocular measurements, meaning that each color was presented once in front of each eye; red–red and green–green for the binocular measurements). The results were averaged for those conditions that stimulate the same eye regardless of the different filter combinations.

2.5. MRI data acquisition

Functional magnetic resonance imaging was performed in a 1.5 T (Siemens Magnetom Vision, with a gradient over-drive) using the standard head coil and a gradient echo EPI sequence (11 slices, TE = 69 ms, TR = 3000 ms; FA = 90°, FOV = 200 × 200 mm², voxel size 1.6 × 1.6 × 3–4 mm³). For binocular mapping of area boundaries an alternative sequence was used (16 slices, TR = 2000 ms; FA = 90°, voxel 3.2 × 3.2 × 4 mm³). A T1-weighted 3D magnetization-prepared rapid acquisition gradient echo sequence (MP-RAGE, TR = 9.7, TE = 4 ms, FA = 12°) lasting 8 min was recorded in the same session as the functional measurements for later matching of anatomical coordinates (voxel size 1.0 × 1.0 × 1.0 mm³). An additional T1-weighted 3D data set tuned to optimize the contrast between gray versus white matter was recorded in a separate recording session lasting 24 min (fast low angle shot [FLASH] sequence), for high resolution 3D reconstruction. Visual stimuli were delivered under computer control (Digital DECpc Celebris XL 590 or DELL Inspiron 7500) via a LCD projector (EIKI LC-6000 or Sony VPL XP 20). Visual stimuli were generated using the Microsoft DirectX graphics library. The image was back-projected onto a screen positioned at the foot end of the scanner.

2.6. Imaging experiments

To achieve monocular stimulation, the subjects wore one of the red–green goggles and red or green filters with matched transmittances were placed in front of the projector. Red–green and green–red goggles were switched between sessions. Stimuli were back-projected onto a screen positioned at the foot end of the scanner and spanned 15° × 20°. This large stimulating field was used in order to minimize the possible effects of eccentric fixation in strabismic subjects.

Phase encoded retinotopic mapping was assessed in each subject and included mapping of eccentricity and polar angle (Goebel, Khorram-Sefat, Muckli, Hacker, & Singer, 1998; Muckli, Kohler, Kriegeskorte, & Singer, 2005; Sereno et al., 1995). In the eccentricity mapping experiment, black and white checkerboard patterns were presented in a ring-shaped configuration and were flickered at a rate of 4 Hz. The ring started with a radius of 1° and slowly expanded to a radius of 12° within 96 s. In the polar angle mapping experiment, the checkerboard pattern consisted of a ray-shaped disk segment subtending 22.5° of polar angle. The ray started at the left horizontal meridian and slowly rotated clockwise for a full cycle of 360° within 96 s. Each mapping experiment consisted of four repetitions of a full expansion or rotation, respectively. Each subject participated in two monocular mapping sessions. Four subjects (EM, RK, KSM, and PZ) participated additionally in a binocular mapping session. Binocular mapping included 10 repetitions of the rotating ray-shaped stimulus and seven repetitions of the expanding ring, each cycle lasting for 64 s.

2.6.1. Imaging experiment A (block presentation)

In a first imaging experiment, the grating stimuli were presented in a predetermined sequence. With the exception of subject MM, each of the eight subjects participated in two fMRI sessions, each of them including the monocular mapping of retinotopic coordinates (polar angle and eccentricity), a 3D anatomical mapping and the assessment of monocular response sensitivity to gratings of four different spatial frequencies (0.5, 4.0, 8.0, and 16.0 c/deg). These spatial frequencies covered the visible range for the dominant eyes of all subjects and included at least one suprathreshold spatial frequency for the amblyopic eye of all subjects. Gratings of a given spatial frequency were presented for periods of 24 s and alternated between horizontal and vertical every 2 s. Each stimulus sequence was followed by 24 s of fixation, after which the other eye was stimulated with a grating of the same spatial frequency. Gratings were presented once in ascending and once in descending order of spatial frequency, such that in each experimental session, each eye was stimulated twice at a particular spatial frequency. Subject MM participated in four fMRI sessions. Since there was no difference between ascending and descending conditions and between sessions, the data were collapsed.

2.6.2. Imaging experiment B (event-related design)

To control for possible effects of expectation in the block design used in the previous experiment, four of the amblyopic subjects included in the previous experiment (the strabismic amblyopes KSM and PZ and the anisometropic amblyopes EM and RK) and four control subjects were tested in a second imaging experiment, using an event-related design. High-contrast (86%) square-wave grating stimuli of three spatial frequencies (6, 12, and 18 c/deg) and two orientations (horizontal and vertical) were presented in a pseudo-random sequence (predetermined by a random generator), interleaved with "flicker" stimuli (blank screens of two different mean luminances). Presentation of each stimulus lasted 2 s, interstimulus intervals varied between 2 and 8 s. Each testing session included 41 grating and 80 blank presentations. The subjects were tested monocularly, using the color goggles described above. One testing session lasted about 10 min, during which the colored filters in front of the projector were switched three times, to allow for stimulation of each eye for two blocks of about 2.5 min. Two testing sessions were performed for each subject,

during which the sequence of monocular stimulation was counterbalanced (LRRL or RLLR). Three-dimensional anatomical mapping, as well as mapping of polar and eccentricity coordinates, were performed for each subject in each experimental session, using the same protocol as in the imaging experiment A.

2.7. Data analysis

Data were analyzed with BrainVoyager 2000—BrainvoyagerQX (BrainInnovation, Maastricht, Netherlands) and included removal of low-frequency drifts, 3D motion detection and correction, determination of Talairach coordinates, multiple regression analysis, cortex reconstruction, inflation and flattening. For the retinotopic mapping experiments we applied a cross correlation analysis. We used the predicted hemodynamic signal time course for the first 1/8 of a stimulation cycle ($= 45°$ in the polar mapping experiment) and shifted this reference function successively in time (time steps correspond to the recording time for one volume $= TR$) (Goebel et al., 1998). Sites activated at particular eccentricities and polar angles were identified through selecting the lag value that resulted in the highest cross-correlation value for a particular voxel. The obtained lag values at particular voxels were encoded in pseudo-color on corresponding surface patches (triangles) of the reconstructed cortical sheet. In the group analysis pixels were included into the statistical map if the obtained multiple correlation value was significant at an alpha level of 0.05. *P* values were corrected for multiple comparison using cortex-based Bonferroni adjustment, i.e., the number of voxels included for correction were limited to the number of gray matter voxels (approximately 38400).

Retinotopic mapping experiments were analyzed with a lowered threshold $r > 0.14$ and were restricted to the occipital cortex. Individual analysis followed the retinotopic mapping and was restricted to the functionally defined borders of visual areas for the region of interest (ROI)-statistics (see below) or to the occipital cortex for the analysis of contrasts. Based on the polar angle mapping experiment, the boundaries of retinotopic cortical areas V1, V2, V3, VP, V3A, and V4v were estimated on the flattened cortical surface (see below). Time courses of the dorsal, ventral, left, and right part of a retinotopic area were averaged geometrically. Individual ROI-time-courses were averaged over subjects and combined to bar plots.

The results of the blocked design imaging experiment A were analyzed with a multiple regression model consisting of four predictors for dominant- (d) and amblyopic- (a) eye stimulation at low (l: 0.5 and 4 c/deg) and high (h: 8 and 16 c/deg) spatial frequency (thus: dl, al, dh, and ah). The overall model fit was assessed using an *F* statistic. The relative contribution of two of the four predictors $RC = (b1 - b2)/(b1 + b2)$ was visualized with a red–yellow–blue–green pseudo-color scale (*b*1 and *b*2 corresponding to dl and al or to dh and ah). The middle values yellow and blue correspond to minimal differences. This color coding was chosen in order to enable comparisons with the results of published studies of our group (Goebel et al., 1998; Linden, Kallenbach, Heinecke, Singer, & Goebel, 1999). Contrast maps were used for the visualization of individual results. Contrast maps ignore regions with identical contribution of *b*1 and *b*2 ($p > 0.2$) and indicate higher activity in pseudo-color scale pink–red for higher activity during amblyopic eye stimulation or green–blue for higher activity during dominant eye stimulation, where pink and green indicate small contrasts and red and blue indicate significant contrasts ($p < 0.05$).

The results of the event-related experiment B were analyzed with a multiple regression model (GLM) consisting of seven predictors: three for dominant- (d), three for amblyopic- (a) eye stimulation at 6, 12, and 18 c/deg, and one for luminance flash conditions. Contrast maps were calculated on individual data. The regions responding stronger for any or all dominant eye conditions as compared to the amblyopic eye were highlighted.

Statistical maps were superimposed onto the original functional scans and incorporated into the high-resolution 3D MRI data sets through interpolation to the same resolution (voxel size: $1.0 \times 1.0 \times 1.0$ mm). This allowed us to produce 3D-reconstructions of the brain with superimposed 3D statistical maps. Coregistration of the respective data sets is based on the Siemens slice position parameters of the $T2^*$-weighted measurement (number of slices, slice thickness, distance factor, Tra-Cor angle, FOV, shift mean, off-center read, off-center phase, in plane resolution) and the T1-weighted 3D MP RAGE measurement (number of sagittal partitions, shift mean, off-center read, off-center phase, and resolution). In order to compare activated brain regions across sessions, anatomical and functional 3D data sets were transformed into Talairach space. Results were visualized by superimposing 3D statistical maps on reconstructions of the cortical sheet.

The recorded high resolution T1-weighted 3D recordings were used for surface reconstruction of both cortical hemispheres of each subject (for details see Kriegeskorte & Goebel, 2001). Results of the group analysis were presented on inflated surface reconstructions of the MNI-template brain (courtesy of the Montreal Neurological Institute). The white/gray matter border was segmented with a region-growing method preceded by inhomogeneity correction of signal intensity across space. The borders of the two resulting segmented subvolumes were tessellated to produce a surface reconstruction of each cortical hemisphere. The resulting surface was used as the reference mesh for projecting functional data on folded, inflated or flattened representations. A morphed surface always possesses a link to the folded reference mesh so that functional data can be shown at the correct location of an inflated as well as flattened representation. This link was also used to keep geometric distortions to a minimum during inflation and flattening through inclusion of a morphing force that keeps the distances between vertices and the area of each triangle of the morphed surface as close as possible to the respective values of the folded reference mesh.

3. Results

3.1. Contrast sensitivity

3.1.1. Individual results

The monocular contrast sensitivity curves of the normal subjects were identical in the two eyes and, for the younger subjects LC, NT, and TS, they fell in the upper range or slightly above the upper limits of the Vistech norms. For the elderly subject EB, the monocular contrast sensitivity values fell in the lower range of the Vistech norms (not illustrated). Individual contrast sensitivities of the amblyopic subjects revealed clear losses in the amblyopic eyes, involving either all spatial frequencies (the anisometropic subjects MaM and EM, the strabismic subjects KG and RS), or only the medium and high spatial frequencies (the anisometropic subjects MM and RK and the strabismic subjects PZ and KSM; see lower rows in Figs. 1A and B).

3.1.2. Group data

The averaged binocular and monocular contrast sensitivity of the control subjects and the two groups of selected amblyopic subjects is shown in Figs. 2A–C. For the control subjects (Fig. 2A), mean contrast sensitivity was in the upper range of the Vistech norms. Binocular values were slightly higher than monocular values. In both strabismic and anisometropic amblyopes, monocular contrast sensitivity of the non-amblyopic eyes was identical to the binocular contrast sensitivity and both fell in the upper range of the Vistech norms (Figs. 2B and C). The averaged contrast sensitivities of the normal, respectively amblyopic eyes of the strabismic and anisometropic amblyopes were remarkably similar (compare Figs. 2B and C).

3.2. Psychophysics: Psychometric functions

The psychometric functions relate percent correct responses to the spatial frequency of high-contrast square-wave gratings. The gratings were viewed through red–green filters made of the same material that was later used in the imaging experiments. Psychometric functions are shown for the dominant and the non-dominant eye, averaged over the responses to horizontal and vertical gratings and to gratings seen through the red and green goggles.

3.2.1. Individual results

The monocular grating acuity was defined as the spatial frequency yielding 75% correct responses. For control subjects, grating acuity was very similar in the two eyes and ranged between 36 c/deg (subject NT) and 20 c/deg (the elderly subject EB), averaging about 24 c/deg (not illustrated). The non-amblyopic eyes of the anisometropic or strabismic amblyopes showed psychometric functions and response latency curves similar to those of the normal subjects. Grating acuity ranged between 20 c/deg for MaM and 32 c/deg for RS (see upper rows in Figs. 1A and B).

All four anisometropic amblyopes had subnormal psychometric functions and response latency curves (upper row in Fig. 1A), when tested with their amblyopic eyes. The densely amblyopic subject MaM showed an interocular grating acuity difference of about two octaves; for EM and MM, the difference in grating acuity between the two eyes was greater than one octave. Even the mildly amblyopic subject RK showed a consistent impairment in his amblyopic eye. These deficits were similar to the deficits in contrast sensitivity (compare the upper and lower rows in Fig. 1A) and Snellen acuity (Table 1) of the same subjects.

The psychometric functions of the four strabismic amblyopes (Fig. 1B) dissociated from their Snellen visus and contrast sensitivity functions. In the densely amblyopic subjects KG and RS, grating acuities and response latencies were definitely subnormal, and so were their contrast sensitivities. By contrast, in the moderately amblyopic subjects KSM and PZ, grating acuity losses, latency increases and contrast sensitivity deficits were much less pronounced than would be expected from their orthoptic data (Table 1), thus confirming previous results (Hess & Howell, 1977; Hilz, Rentschler, & Brettel, 1977).

3.2.2. Group data

Fig. 2 shows the averaged data of the control group (Figs. 2D–G) and the two groups of experimental subjects (anisometropes in Figs. 2E–H, strabismic in Fig. 2FI). For the normal subjects, the psychometric functions and the response latency curves were identical in the two eyes. The psychometric functions of the dominant eyes of the amblyopic subjects were similar to those of the normal subjects and showed no differences between groups. The psychometric functions of the amblyopic eyes of the two groups of amblyopic subjects showed about the same amount of deficit, thus justifying a quantitative comparison between the two groups. Response latencies increased with increasing spatial frequency (Figs. 2G–I) and were consistently larger in amblyopic than in the fellow eyes (Figs. 2H and I).

3.2.3. Psychophysics: Control experiments
3.2.3.1. Effect of stimulus color.
To control for the effect of the colored filters on psychometric functions, the results of all tested subjects were averaged, separated by color (Figs. 3A and B). There was no difference in the psychophysical results for the red as compared to the green filter. Thus, we can be confident that the choice of the filter combination did not have an influence on the psychophysical results of the subjects. Therefore, the results obtained with filters of different colors were pooled.

3.2.3.2. Effect of stimulus orientation.
In Figs. 3C and D, the results of all subjects are pooled according to the orientation of the gratings (vertical vs. horizontal). No differences or only a very slight advantage of the horizontal gratings is apparent for the higher spatial frequencies. This might reflect the "vertical effect," known to occur in strabismic amblyopes (Sireteanu & Singer, 1980). In the following, the
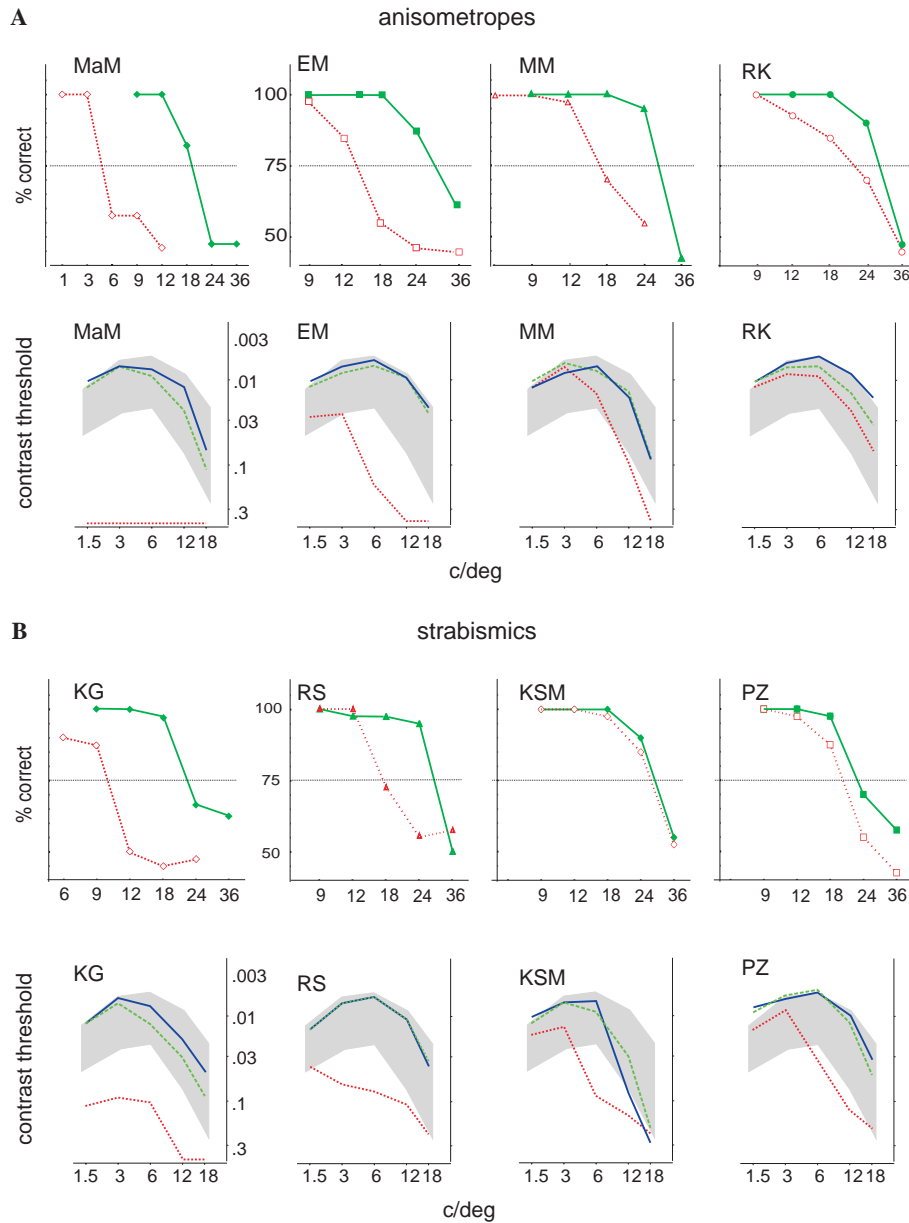
Fig. 1. Individual contrast sensitivities and individual performance of orientation discrimination for the group of anisometropic amblyopes (A) *and strabismic amblyopes* (B). Upper panels: Percent correct responses and response latencies are plotted as a function of spatial frequencies for the monocular stimulations (red dotted: amblyopic eyes; green solid lines: dominant eyes). Fifty percent correct corresponds to chance responses. The horizontal line indicates the 75% threshold. Lower panels: Individual contrast thresholds are shown for binocular vision (solid blue), for dominant eye (dashed green), and amblyopic eye (dotted red) stimulation of all experimental subjects. Normal contrast sensitivity as provided by the Vistech norms is indicated by gray shading.

results obtained for different stimulus orientations shall be pooled.

3.3. Magnetic resonance imaging: Experiment A (block design)

3.3.1. Retinotopic mapping of amblyopic subjects

Individual mappings are shown in Figs. 4 and 5 for four representative subjects (the anisometropic amblyopes MM and EM and the strabismic amblyopes KG and KSM). These subjects show a moderate amblyopia (corrected Snellen visus ranging from 0.20 to 0.60) and stable fixation

(foveolar in the two anisometropic amblyopes, nasal in the two strabismics), thus avoiding potential confounds due to extremely deep acuity loss or unstable fixation.

In these four subjects, maps were obtained not only with monocular but also with binocular stimulation. The two mapping procedures yielded very similar results. However, binocular mapping procedures were optimized in some technical respects (number of repetitions, TR, and voxel-resolution) that improved the resolution of maps. Thus, in these four subjects we relied on the binocular maps and in the others we averaged the monocular maps across sessions to increase reliability. Through this procedure we succeeded
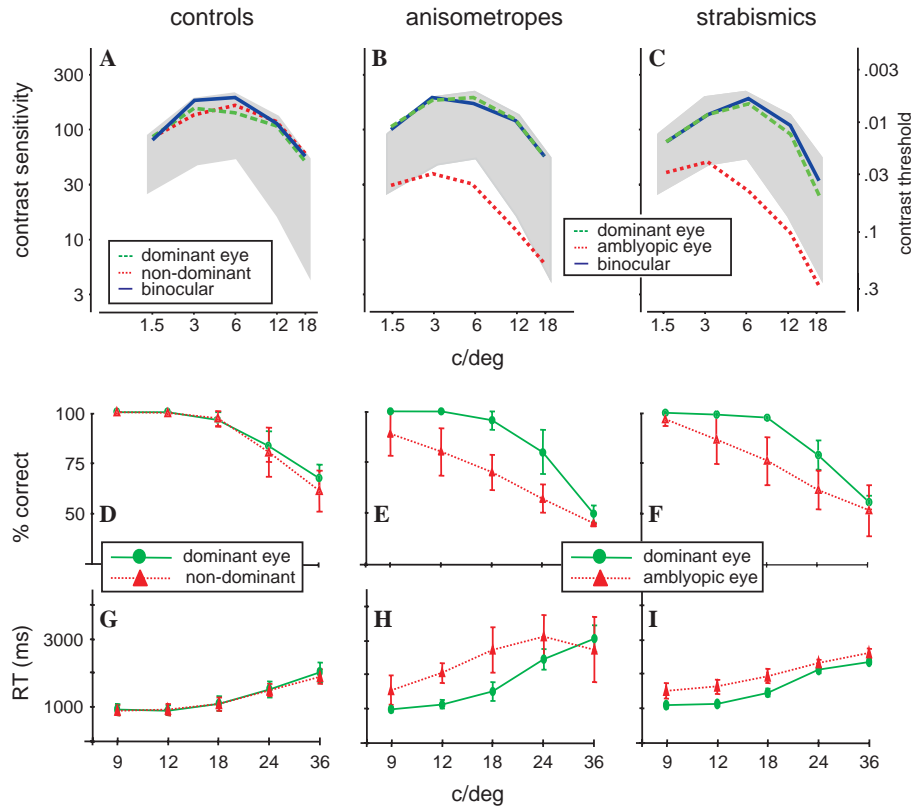
Fig. 2. Group averaged contrast sensitivity curves and psychometric functions for control subjects and for anisometropic and strabismic amblyopes. Monocular and binocular contrast sensitivity for near vision is shown at different spatial frequencies and is averaged for the selected groups of control subjects (A), for anisometropic amblyopes (B), and for strabismic amblyopes (C). Contrast sensitivity functions were acquired using Vistech charts. Normal contrast sensitivity as provided by the Vistech norms is indicated by gray shading. Contrast sensitivity and contrast thresholds are shown for the dominant eye (green dashed), the amblyopic or non-dominant eye (red dotted), and for binocular vision (blue solid). Psychometric functions are averaged for the group of control subjects (D), anisometropic (E), and strabismic amblyopes (F). Performances are plotted as a function of spatial frequency for the dominant eye in green (solid) and for the non-dominant eye or the amblyopic eye in red (dotted). Response latencies are shown as a function of spatial frequency for control subjects (G), for anisometropic- (H) and for strabismic amblyopes (I). Color codes indicate the dominant, non-dominant, and amblyopic eye.
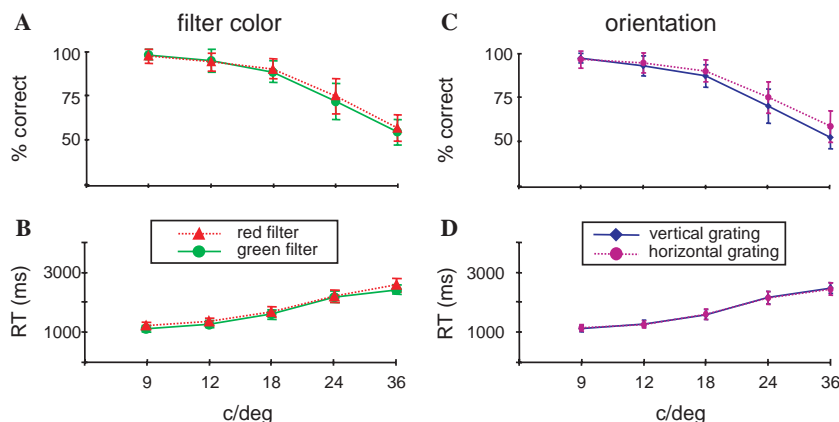
Fig. 3. Control experiments. The effect of filter color (A and B) and grating orientation (C and D) on the results of the psychophysical experiments. Psychometric curves (A and C) and response latencies (B and D) both shown as a function of spatial frequency. Data were pooled over all subjects.

to map areas V1, V2, V3, V3a, and VP, V4/V8, and LOC in all 16 hemispheres of the amblyopic subjects.

The representation of the vertical meridian delineates V1 from V2 and V3 from V3a in the dorsal visual areas and VP from V4 in the ventral visual areas. In Figs. 4 and 5 the representation of the lower vertical meridian appears in red

and for the vertical meridian in the upper visual field in green. The horizontal meridian separates V2d from V3 and V2v from VP, respectively. Here the colors yellow and blue refer to lower (yellow) and upper (blue) visual field representations, respectively (for color codes see upper panels in Fig. 4). The estimated borders are indicated by hand drawn
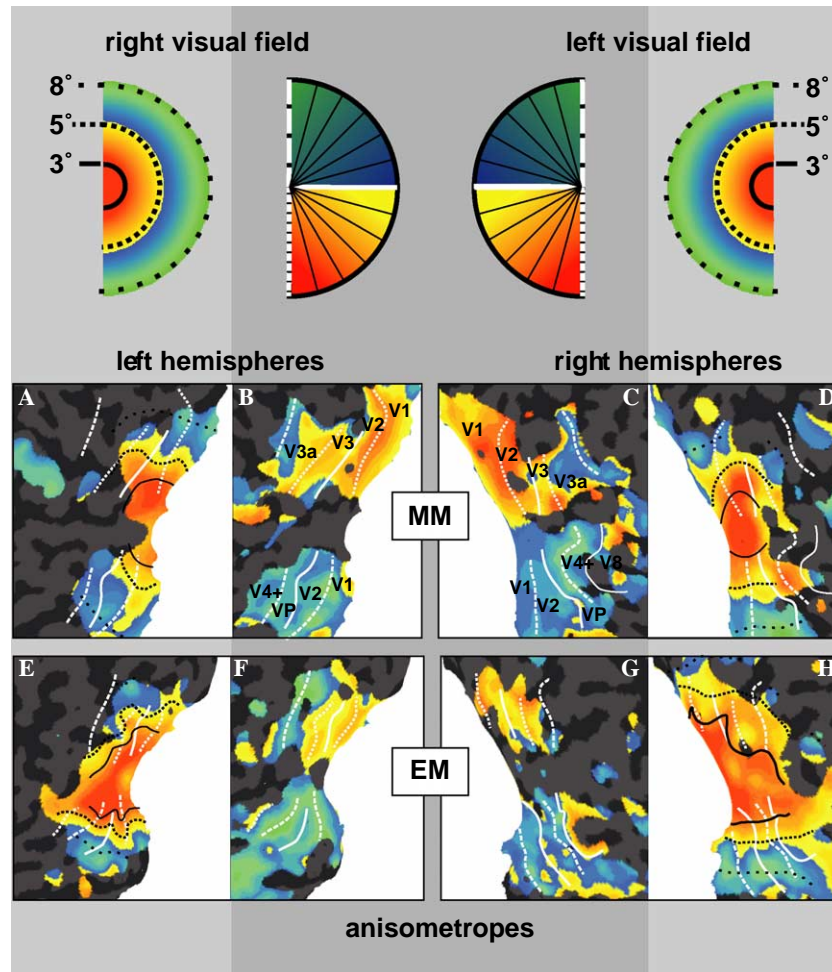
Fig. 4. Phase encoded retinotopic maps of two anisometropic amblyopes. Top row indicates color codes for each column (right eccentricity, right polar-angle, left polar-angle, left eccentricity). Maps are shown on flattened representations of the cortical sheet. The tissue is cut along the horizontal meridian of V1, which follows roughly the calcarine sulcus. The time point of a region's highest activity determines the color code at that location and corresponds to the indicated eccentricity or polar angle stimulation. Maps are shown for subject MM (A–D) and for subject EM (E–H). Dark lines indicate eccentricity lines at approximately 3°, 5°, and 8° eccentricity. White lines indicate area borders (dashed lines—vertical meridian; solid lines—horizontal meridian).

white lines (continuous lines for horizontal meridian, dotted lines for lower vertical meridian, dashed lines for upper vertical meridian).

Areas V3a and V8 are clearly characterized by a complete hemifield representation. However, the anterior boundaries to V3a and V8 are difficult to map. One reason is that we did not cover the whole region in all measurements with our slab thickness of 3.3 cm, another reason is that many repetitions are needed to reveal retinotopic maps beyond the level of V3a (Tootell & Hadjikhani, 2001; Tootell et al., 1997; Tootell, Hadjikhani, Mendola, Marrett, & Dale, 1998). We suspect that the borders of V3a to presumed V7 and other functional regions in the superior–occipital sulcus as well as the border to V8 in the fusiform gyrus were not mapped reliably. We could ascertain, however, that the foveal representation of V8 lies ventrally to the foveal representation of V1–V3 in most subjects. In cases were we could not delineate V4 and V8 we used V4+ to label the whole complex. The lateral occipital cortex (LOC) was not mapped retinotopically as it exhibits only a

crude retinotopic organisation. We refer to it as the region around the lateral occipital sulcus, that is located posteriorly on the lateral aspect of the fusiform gyrus and is not belonging to any of the regions exhibiting retinotopic maps (Malach et al., 1995).

3.3.2. Cortical activation maps: Individual results

In the following, the individual activation maps shall be illustrated for the four selected representative subjects: the anisometropic amblyopes MM and EM and the strabismic amblyopes KSM and KG (see Figs. 6A–C and 7A, B). The orthoptic details of these four subjects were presented in Table 1, the contrast sensitivities and psychometric functions in Fig. 2, their retinotopic maps in Figs. 4 and 5. The remaining subjects were analyzed in the same way and contributed to the averaged bar plots in Figs. 6D and 7C. The retinotopically defined borders of visual areas were used to extract ROI time courses. These time courses were shown individually and also averaged for all four anisometropes (Fig. 6D) and all four strabismics (Fig. 7C). To enable a
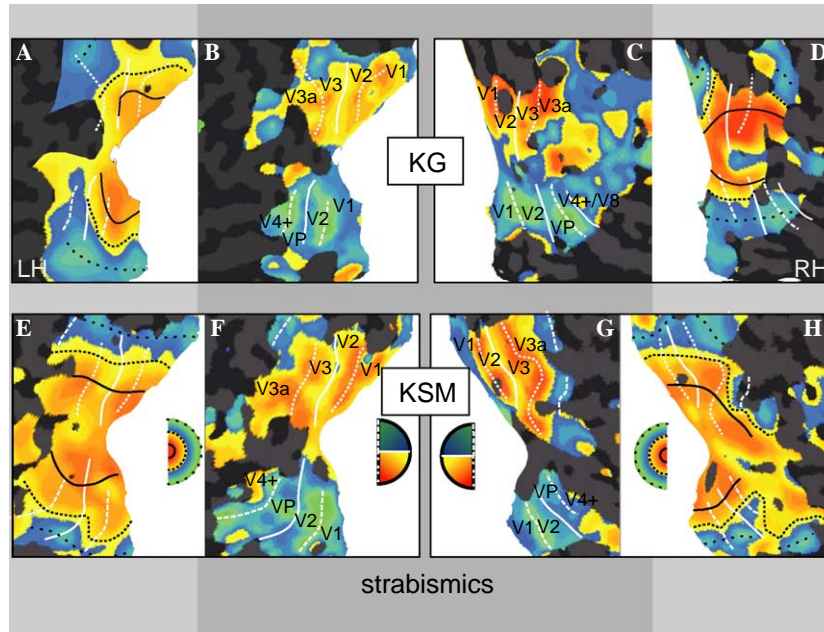
Fig. 5. Retinotopic mapping results for two strabismic amblyopes. Phase encoded maps refer to the same color codes as in Fig. 4. Top row shows maps of KG (from left to right): eccentricity map of the left hemisphere (A), left hemispheric polar-angle map (B), right hemispheric polar-angle map (C), right eccentricity map (D). Maps of KSM are shown (E–F) in the same sequence. Black and white lines as in Fig. 4.

better visualization of the results of the selected subjects, cortical activation was averaged for the gratings with lower (0.5 and 4 c/deg) and higher spatial frequencies (8 and 16 c/deg), respectively.

3.3.2.1. Anisometropic amblyopes. For the dominant eye of the anisometropic subjects, the cortical responses to low spatial frequency gratings (0.5 and 4 c/deg) were similar and always stronger than responses to high spatial frequencies (8 and 16 c/deg; Fig. 6D). This is in good agreement with the spatial frequency dependent activation levels reported in humans (Singh, Smith, & Greenlee, 2000) and monkeys (Foster, Gaska, Nagler, & Pollen, 1985) that have a maximum for gratings of 1–4 c/deg in V1 and for slightly coarser gratings in areas V2, V3, and VP (Singh et al., 2000). Paradoxically, for the amblyopic eyes, which exhibited differential impairment for high spatial frequencies, the differences between responses to high and low frequencies were less pronounced in most visual areas except LOC.

To assess differences in cortical activation most closely related to the amblyopic deficit, we first compared the responses to the two eyes at high spatial frequencies (8 and 16 c/deg) on flattened hemispheres for the two representative subjects with a moderately dense amblyopia and foveolar fixation (EM and MM; Figs. 6A and C). Regions activated more strongly from the normal than the amblyopic eye cover large parts of the occipital cortex (green and blue in Fig. 6A). In subject MM differences were maximal in V3a, V4+, and LOC of both hemispheres (Figs. 6A and B, blue region; $F[1, 507] > 5$; $p < 0.05$) and for subject EM in V3a, V4+, and LOC of the left hemisphere, which is ipsilateral to the amblyopic eye (Fig. 6C, $p < 0.05$). There are three

ROI-time courses exemplifying our findings for MM's left hemispheric V4+, V3, and V1 in Fig. 6B (numbered 1–3).

Averaged over all anisometropic subjects, the areas showing consistently stronger responses to the normal eye at high spatial frequencies were areas V4+ and LOC (Fig. 6D, green bar higher than pink bar). Surprisingly, however, in lower visual areas we observed broad activation bands that responded more strongly to the amblyopic eye than to the normal eye (shown in pink in Figs. 6A and C). For subjects MM and EM these bands were confined mainly to V1 and V2. However, in EM's right dorsal hemisphere, these regions were seen in V3 and V3a rather than in V1 and V2. With small variations like those observed in EM's right hemisphere, subjects RK and MaM exhibited the same pattern of activation as MM and EM: there were regions in V1 and V2 that responded more strongly to the amblyopic than to the normal eye while in areas V4+ and LOC responses were always stronger to the normal than to the amblyopic eye. At low spatial frequencies all regions except parafoveal V1 and V2 showed a clear attenuation of responses evoked from the amblyopic eye (compare red and blue bars in Fig. 6D).

3.3.2.2. Strabismic amblyopes. In all visual areas, responses were again stronger when evoked with low than with high spatial frequency gratings. In areas VP and V4+ responses evoked through the amblyopic eye were much weaker than those evoked through the normal eye and because of the low amplitude of these responses, differences between low and high spatial frequency gratings could not be determined. In extrastriate regions, the activation patterns obtained with high spatial frequency gratings resembled in
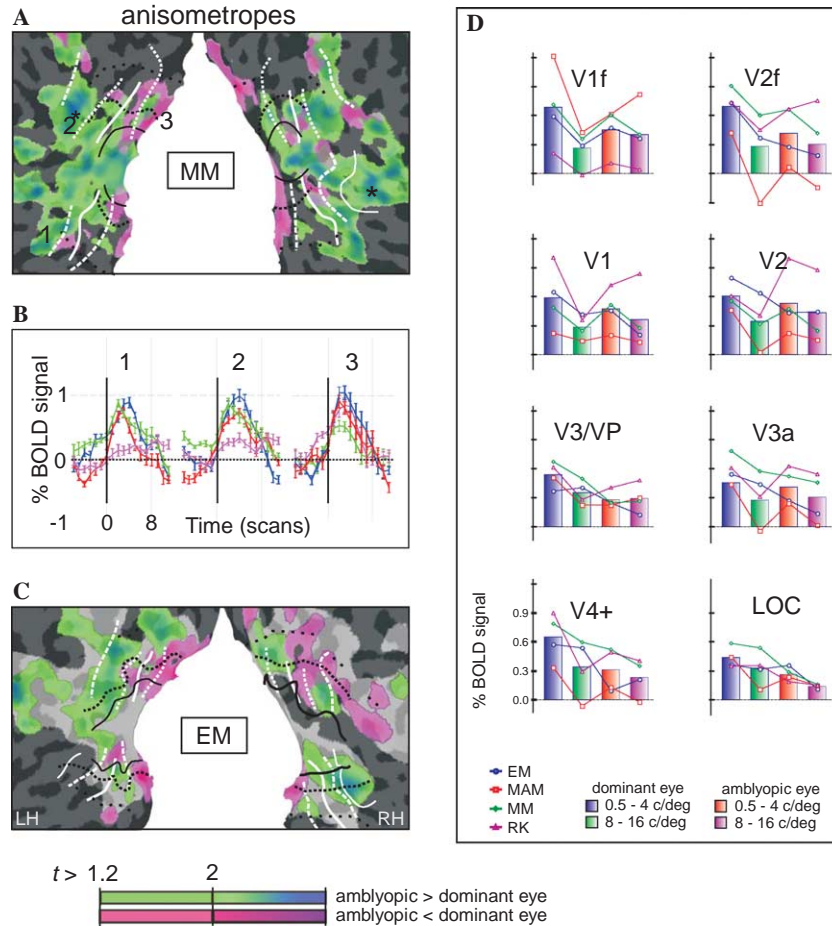
Fig. 6. Cortical activation patterns of anisometropic amblyopes (block design; experiment A). Monocular activation patterns for subject MM (A) and EM (C) on flattened representations of left and right occipital cortex. Borders of visual areas and their eccentric representations are indicated with white and black lines derived from retinotopic maps (cf. Fig. 4). Contrast maps indicate regions that respond more to dominant-eye stimulation in colors green–blue or more to amblyopic-eye stimulation in colors pink–red. Examples of signal time courses are taken from subject MM (A) and are presented in (B) for visual areas V4-ventral (1), V3a-dorsal (2), and V1-dorsal (3). Whiskers in (B) indicate standard error of means across repetition of same condition within subject MM. Group-averaged mean responses for all anisometropes are presented in (D) for visual areas: V1, V2, V1f (fovea only), V2f (fovea only), V3 and VP, V3a, V4+, and LOC. Mean individual responses are indicated for each subject.

many aspects those of the anisometropic subjects: Responses to stimulation of the amblyopic eye were attenuated in areas V3, V3a, VP, V4+/V8, and LOC.

In the lower visual areas, activation patterns evoked with high spatial frequency gratings were more variable than in anisometropic amblyopes. In V1 responses were strong but interocular differences were inhomogeneous. Again, some subregions showed stronger activation after stimulation of the amblyopic eye. Unlike in the anisometropic amblyopes, other subregions responded more vigorously to the normal eye. In three subjects (KG, PZ, and RS) there was an overall tendency for stronger responses to the amblyopic eye in regions of early visual areas representing the peripheral visual field (e.g., KG in Fig. 7B). In one subject (KSM, Fig. 7A), the amblyopic eye evoked stronger responses in the foveal representation of V1 than the normal eye. Overall, however, activation of the extrastriate cortical areas became progressively weaker when stimulated through the amblyopic eye of the strabismic subjects.

3.3.2.3. Overall cortical activation (group data). In the matched groups of anisometropic and strabismic amblyopes, cortical activation exhibited clear interocular differences—especially for gratings with higher spatial frequencies (8 and 16 c/deg). These group results are summarized in Fig. 8.

The largest interocular differences were observed in occipito–temporal regions located at the posterior end of the occipito–temporal–sulcus. In these areas, the responses evoked through the amblyopic eye were consistently reduced. These regions extended laterally into the inferior temporal gyrus and ventrally into the fusiform gyrus (green–blue regions in Fig. 8). Strong and highly significant ($p < 0.001$ for all constellations) activation differences were observed both at high (8 and 16 c/deg) and low (0.5 and 4 c/deg) spatial frequencies for both anisometropic (high frequency: $t(507) = 4.7$, $p < 10^{-5}$; low frequency: $t(507) = 7.2$, $p < 10^{-7}$) and strabismic amblyopes (high frequency: $t(507) = 4.9$, $p < 10^{-6}$; low frequency: $t(507) = 5.6$, $p < 10^{-7}$).
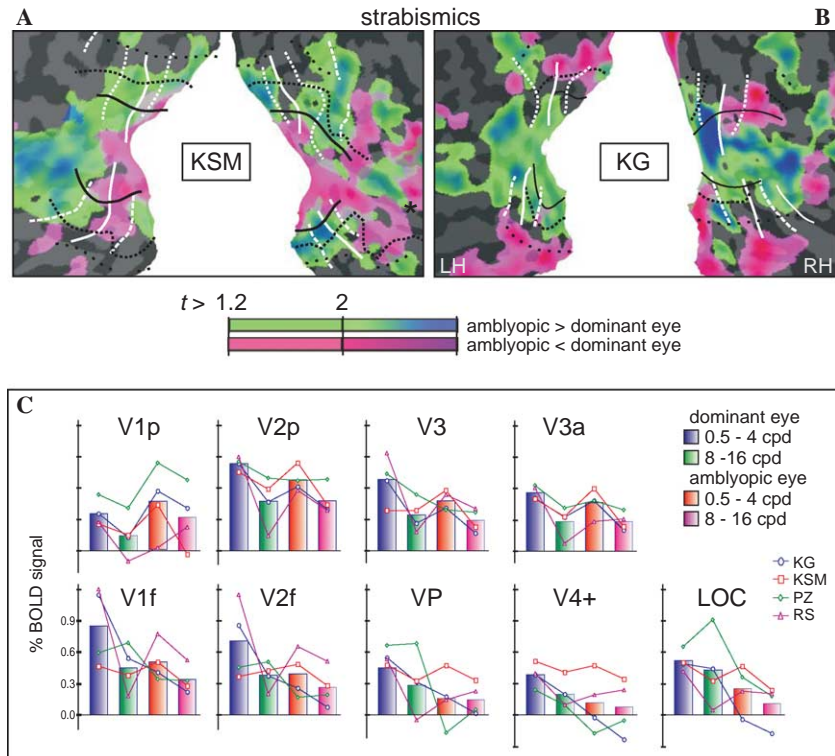
Fig. 7. Cortical activation patterns of strabismic amblyopes (block design; experiment A). Monocular activation patterns for subject KSM (A) and KG (B) (color scale as described for Fig. 6). Cortical sheets and retinotopic maps are derived from Fig. 5. Group-averaged mean responses for all strabismics from predefined visual areas (C): V1p (peripheral), V1f (fovea), V2p (peripheral), V2f (fovea), V3, VP, V3a, V4+ (possibly including V8), and LOC. Mean individual responses are indicated for each subject.

In Fig. 8, relative contribution maps are shown for regions that are significantly activated in any of the tested conditions ($p < 0.05$; Bonferroni corrected for multiple comparison). The color scale indicates to which eye the region responds better. Blue and yellow indicate insignificant variations ($t < 2.6$, $p > 0.01$), and red and green significant differences ($t > 2.6$, $p < 0.01$).

Early visual areas in the medial region of the occipital lobe, located around the calcarine sulcus, showed a distinctly different pattern of activation. At high spatial frequencies, activation was stronger for the amblyopic than the normal eye, this interocular difference being more pronounced for anisometropic (red color around sulcus calcarinus in Fig. 8) than for the strabismic subjects (yellow and red region in Fig. 8 top row). At low spatial frequencies, activation in this region was similar for the two eyes (blue and yellow colors). In strabismic amblyopes, stronger responses to the amblyopic eye were also observed in anterior parts of the sulcus calcarinus, suggesting that the peripheral sections of early visual areas might respond more strongly to the amblyopic eye than to the normal eye.

3.4. Magnetic resonance imaging: Experiment B (event-related design)

The previous experiment has demonstrated that cortical activation through the amblyopic eyes is progressively attenuated towards higher cortical levels, thus confirming

our original hypothesis. However, the lack of an amblyopic deficit in early cortical areas (and the occasional higher activation evoked by the amblyopic eyes in parts of the early cortical areas), is intriguing. We wondered whether this effect might have been due to individual differences in the subjects' performance or to the subjects' expectation in the block design used in the previous experiment.

Ress, Backus, and Heeger (2000) and Ress and Heeger (2003) reported strong activity in V1 following an acoustic cue which usually preceded a low-contrast visual stimulus, even for trials in which the target was not presented. They interpreted this activation in absence of visual stimulation as a result of expectation. Our question was whether, similar to an acoustic cue, a block design might build up expectation, if the delay between stimulus presentations was constant. In an event-related experiment, the subjects are not able to predict the occurrence of a stimulus.

In this experiment, four of the eight subjects tested previously (the anisometropic amblyopes EM and RK and the strabismic amblyopes KSM and PZ) were tested with an event-related design. Only three spatial frequencies (6, 12, and 18 c/deg) were used, interleaved with blank screens of two slightly different luminance levels. The stimuli were presented after variable intervals and had variable spatial frequencies and orientations.

The results of the four individual subjects included in the event-related imaging experiment B are shown in Figs. 9A–C. Overall activity maps are shown in Fig. 9A and time courses
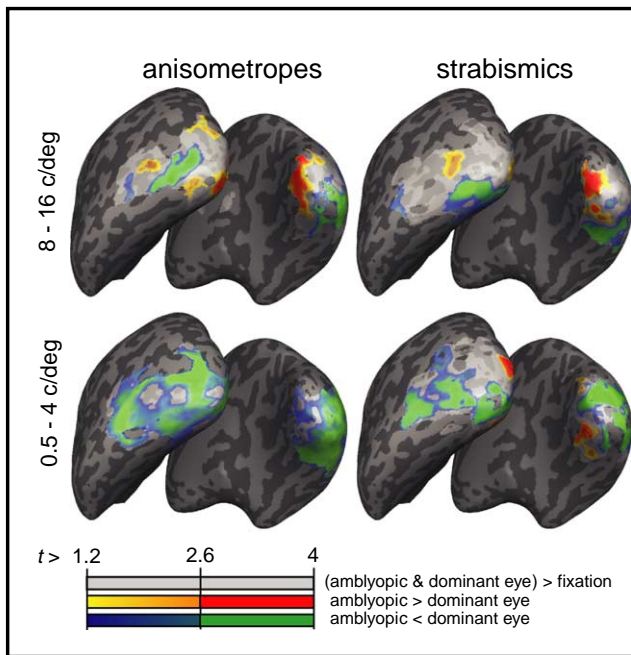
Fig. 8. Group analysis of cortical activation of anisometropic and strabismic amblyopes (experiment A). Relative contribution maps are derived from GLM-analysis and shown superimposed on inflated representations of template brain hemispheres. Gray-scale contours reflect the tissue curvature (dark: concave, light: convex). Maps are given for high (top row) and low (bottom row) spatial frequency and for anisometropic (left column) and strabismic amblyopia (right column) separately. Light gray shading indicates the region from which EPI images were acquired in all subjects, with at least a minimal increase of signal during visual stimulation ($t > 1.2$). Colored regions show a significant increase of activation relative to fixation ($p < 0.05$; after Bonferroni correction for multiple comparisons). The colors indicate contrast between the respective eyes. Statistically significant are the red and green colors ($t > 2.6$; $p < 0.01$). Yellow and blue indicate only insignificant differences between the two eyes.

for selected extrastriate regions in Fig. 9B. The psychophysical data collected during the fMRI experiments (manual reaction times and percent correct responses) are shown in Fig. 9C.

3.4.1. Psychometric functions

Psychophysically, all subjects responded at or close to 100% for the grating with the lowest spatial frequency (6 c/deg). With the dominant eyes, the subjects still performed at 100% for the medium spatial frequency but responses were clearly reduced for the highest available spatial frequency (18 c/deg; see green columns in the lower panels in Fig. 9C). With the amblyopic eyes, responses were already reduced for the medium spatial frequency and almost completely abolished for the highest spatial frequency (red columns in Fig. 9C). For both eyes, response latencies increased with increasing spatial frequency. Manual reaction times were higher for the amblyopic eyes (red lines in the upper panels in Fig. 9C) and, for subjects RK, PZ, and KSM, they exceeded the time limit imposed for response (see Section 2).

3.4.2. Overall cortical activation

In Fig. 9A, retinotopic areas are marked with alternating blue and yellow stripes. In addition, cortical regions show-

ing increased activation through the dominant eyes are highlighted in green color. As seen from the figure, it was not possible to extract clear stimulus impulse functions showing reduced activation through the amblyopic eyes in the early visual areas. The strongest and most reliable differences between responses to dominant and amblyopic eye stimulation were found in the cortical areas V4+/V8, LOC, and in regions in the ventral temporal cortex located anterior to the known retinotopic areas. (These anterior temporal–ventral regions where not covered in the block-design fMRI experiment A.)

3.4.3. Extrastriate cortical activation

Exemplary time courses for the selected extrastriate regions are shown in Fig. 9B, separately for each spatial frequency. There was substantial interindividual variation. All subjects showed clear activations through the dominant eyes at the lowest spatial frequency (6 c/deg), but decreased activations at the higher spatial frequencies (12 and 18 c/deg). For subjects EM, PZ, and KSM, clear responses were obtained for amblyopic eye stimulation at 6 c/deg (always smaller than the activations through the dominant eyes), but markedly reduced or absent activations at the higher spatial frequencies. Subject RK showed the most marked activity loss to amblyopic eye stimulation at the lowest spatial frequency (6 c/deg). For subject EM, a reduction of activation for the amblyopic eye was seen only for the highest spatial frequency (18 c/deg). As in experiment A, there were no consistent differences between strabismic and anisometropic amblyopes.

Thus, all subjects showed clear activity reductions to stimulation of the amblyopic eye in higher-order, extrastriate cortical areas, including areas V4+/V8 and LOC, but no consistent reductions in the early cortical areas, thus confirming the results of the block design fMRI experiment A. Activity reductions in the higher-order cortical areas involved mainly the higher spatial frequencies. In spite of similar tendencies, there was no simple relationship between the cortical activation patterns in these higher cortical areas and the simultaneously measured psychophysical responses.

4. Discussion

4.1. Summary of the results

A consistent finding of this study was that both in anisometropic and strabismic subjects, cortical responses evoked through the amblyopic eye were attenuated in extrastriate visual areas, including LOC and V4+/V8. This attenuation was more pronounced for higher than for lower spatial frequency gratings. In contrast, lower tier areas V1 and V2 showed no or only small and mostly foveal attenuation of responses evoked from the amblyopic eye. Overall activation patterns in lower tier areas were more variable and patchy in strabismic than in anisometropic amblyopes, while in higher tier areas the patterns of activation were
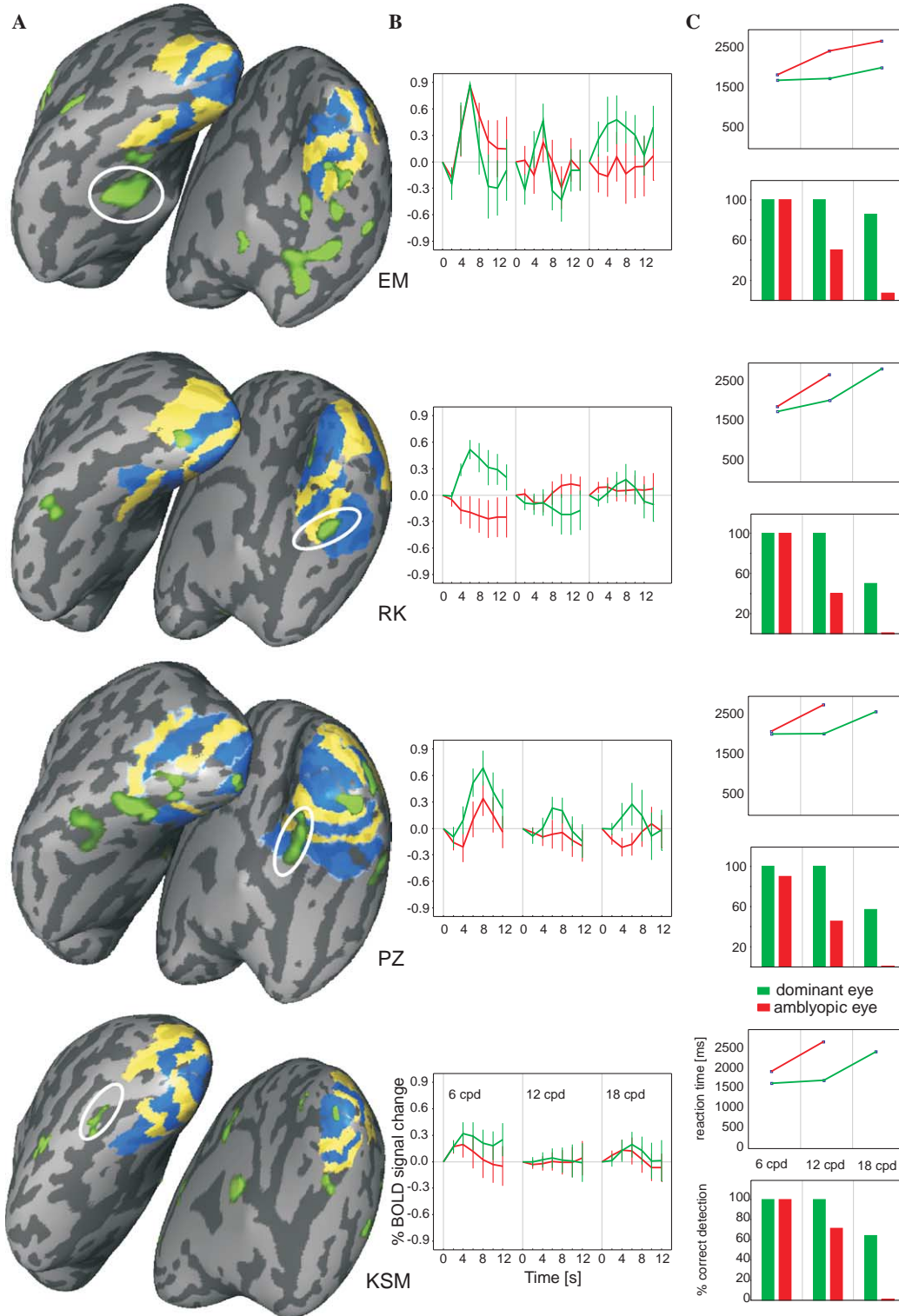
Fig. 9. Individual cortical activation pattern for two anismetropic (EM, RK) and two strabismic (PZ, KSM) subjects (event-related design; experiment B). Contrast activation maps are shown on inflated cortex reconstructions (A) (posterior–ventral view). Green regions indicate activation with higher activation for the dominant eye for one or for all spatial frequencies. Early visual areas as mapped using binocular retinotopic mapping are shown in yellow and in blue (V1, yellow; V2, blue; V3 and VP, yellow; V4 and V3a, blue; V8 or V4+ in blue for RK and PZ). Selected exemplary time courses (B) from area V4+/V8 (for subject RK and PZ), LOC (KSM) and non-retinotopic anterior ventro-temporal region (EM). Individual psychophysical data during fMRI experiments (C) show percent correct detection of oriented gratings at 6, 12, and 18 c/deg (bar plots), and manual reaction time to the respective gratings (line plots). Color codes for all plots: red for amblyopic eye stimulation and green for dominant eye stimulation.

similar in anisometropic and strabismic amblyopes. Occasionally, we found that parts of V1 and V2, and in particular the peripheral regions, responded more strongly to the amblyopic eye.

There was surprisingly little difference between strabismic and anisometropic amblyopes, both in their psychophysical responses and in their cortical activation patterns. While the reduction in contrast sensitivity and grating acuity is known to involve both groups of subjects (cf. Hess & Howell, 1977), results from animal studies suggest a progressive reduction of neural responses in higher cortical areas in strabismic (Roelfsema et al., 1994; Schröder et al., 2002; Sireteanu, 1991; Sireteanu & Best, 1992), but not in anisometropic subjects (Kiorpes et al., 1998). One possible explanation might be found in the selection of our subjects. While our assignment of the subjects to the different groups reflected their aetiology, the age at which microtropia ensued in the anisometropic subjects as well as the amount of ametropia present in early childhood in the strabismic subjects cannot be reconstructed from their history and thus their relative impact on the development of the amblyopic deficit remains unknown.

4.2. Relationship to previous studies

Only few previous imaging studies of human subjects affected by amblyopia investigated activation differences between striate and extrastriate cortex. Response attenuation was reported in extrastriate cortex ipsilateral to the amblyopic eye (Imamura et al., 1997), in the "occipital" cortex of both hemispheres (Kabasakal et al., 1995) and exclusively in "V1" (Algaze et al., 2002; Anderson et al., 1999; Demer et al., 1997, 1988; Goodyear et al., 2000; Lee et al., 2001). The discrepancy between these results and the results of the present study may partly be accounted for by the diversity of stimuli. These consisted of stroboscopic flashes (Demer et al., 1988), motion pictures (Demer et al., 1988), reversing checkerboard patterns (Imamura et al., 1997; Kabasakal et al., 1995), or sinusoidal gratings (Goodyear et al., 2000). Stimuli such as dramatic motion pictures are likely to preferentially activate extrastriate regions while unstructured stimuli such as stroboscopic flashes are expected to drive only lower visual areas and do not seem well suited to reveal amblyopic deficits.

Two recent imaging studies that have adequately separated striate and extrastriate responses in strabismic amblyopes (Barnes et al., 2001; Lerner et al., 2003) deserve special mention. The study of Barnes et al. (2001) revealed a reduction of responses in striate cortex for the amblyopic eye for gratings at low spatial frequencies, which is in good agreement with our findings. With high spatial frequencies, they found again a reduction of responses in early visual areas of strabismic amblyopes. We can confirm this finding only for the foveal representation. In contrast to our study, Barnes et al. (2001) had included a central attention task, which might account for a discrepancy to our finding of relatively strong activation in the periphery of early visual

areas during amblyopic eye stimulation. Further methodological differences are our use of high-contrast gratings and of a large projection screen (15° × 20°) instead of the 22% contrast gratings and the relatively small (5.4° width) stimuli used by Barnes et al. (2001). High contrast gratings are widely used in animal and human psychophysics (Roelfsema et al., 1994), but these stimuli are known to cause less severe deficits in amblyopes (Hess, Pointer, Simmers, & Bex, 2003). Large-field stimuli stimulate parts of the peripheral visual field, which is known to be relatively spared in strabismic amblyopia (Hess & Pointer, 1985; Sireteanu & Fronius, 1981). Good responses of early visual areas might therefore be connected to the use of high-contrast, large-field gratings. In contrast, small stimulation fields in eccentrically fixating strabismic amblyopes might address primarily peripheral, retinotopically non-corresponding cortical areas, thus rendering a direct comparison of the patterns of activity evoked by the two eyes rather difficult.

The recent study of Lerner et al. (2003) reported non-impaired activity in the striate cortex of strabismic amblyopes and a selective impairment in the face-related area in the fusiform gyrus, while building-related regions in the collateral sulcus remained essentially normal. The authors consider that their results might be related to the fact that face processing depends on fine-detail analysis (Hasson, Levy, Behrmann, Hendler, & Malach, 2002; Levy, Hasson, Avidan, Hendler, & Malach, 2001), while building-related processes involve large-scale feature integration. They conclude that their results argue "against a low-level source for the amblyopic deficit and for a disconnection site at a high-order locus." This conclusion agrees with our results. However, it remains to be clarified whether the face-processing deficit in strabismic amblyopes is not secondary to other perceptual deficits like loss of acuity, contrast sensitivity, positional acuity, and crowding. The impairments in the face-processing area might reflect a more general, progressive disconnection of higher-level visual areas, especially those responsible for processing fine spatial details.

Our behavioral tests confirmed impaired processing for high spatial frequency gratings and this perceptual deficit covaried best with the spatial frequency sensitive attenuation of responses in LOC. In the other extrastriate areas this attenuation was less pronounced, as e.g. in V4 of anisometropic amblyopes, or it was not dependent on spatial frequency at all, as in VP and V4+ of strabismic amblyopes. Thus, the best correlation between perceptual impairment and response attenuation was the spatial frequency dependent response attenuation in area LOC. Good correlation between perception of visual objects and LOC activity has also been observed in normal subjects (Amedi, Malach, Hendler, Peled, & Zohary, 2001; Grill-Spector, Kushnir, Hendler, & Malach, 2000; Levy et al., 2001; Malach et al., 1995). A study of Grill-Spector (2001) has shown that activity in LOC is enhanced after recognition performance has been improved by training. Attenuation of LOC activity in amblyopic subjects might therefore be seen as a

consequence of the consistent neglect of signals provided by the amblyopic eye.

4.3. Effects on striate cortex: Possible roles of expectation and attention

The most intriguing finding of this study was that, in both groups of amblyopic subjects, the affected eye did not evoke reduced responses in early visual areas, and occasionally the responses in parts of areas V1 and V2 were even stronger for the affected than for the non-affected eye. This finding was surprising; several possibilities have to be considered for its explanation.

We wondered whether this higher activation might be related to the use of a blocked, instead of an event-related design. Upon blocked presentation, increased activation for higher spatial frequency gratings might be seen as a result of expectation. For several reasons, we do not consider this a likely possibility: (1) the effects were seen regardless whether spatial frequencies were presented in ascending or descending order; (2) it is not clear why expectation should produce enhanced activation for the amblyopic and not for the dominant eye; and (3) it is not clear why these effects should be seen only in the primary, and not in higher-order visual areas. If the lack of an amblyopic deficit in early visual areas were due to expectation, this effect should disappear during an event-related experiment. However, this was not the case: the results of the event-related experiment confirm the results of the block-design experiment, in that they do not indicate a bias in favour of the dominant eye over the amblyopic eye in early visual areas. Although expectation might contribute to the overall signals, it can not explain differential effects.

Another possible explanation for the increased cortical activity in parts of the peripheral visual field regions of amblyopic subjects in lower visual areas might be related to the non-uniform distribution of visual acuity and interocular suppression across the visual field that has been observed in human subjects (Sireteanu & Fronius, 1981; Sireteanu, Fronius, & Singer, 1981) and in monkeys affected by strabismic amblyopia (Horton, Hocking, & Adams, 1999; Thiele, Bremmer, Ilg, & Hoffmann, 1997). It has been suggested that strabismic amblyopia results from chronic interocular suppression that occurs in regions of the visual field where fusion of the signals from the two eyes is not possible (Sireteanu, 1982; Sireteanu & Fronius, 1981). With small squint angles fusion is prevented only in the central but not in the peripheral parts of the visual field, because the larger receptive fields in the periphery permit integration of binocular signals and the development of anomalous correspondence (Sireteanu & Best, 1992; Sireteanu & Fronius, 1989). Thus certain binocular functions such as the perception of motion in depth are preserved in the visual field periphery of strabismic and anisometropic amblyopes (Sireteanu et al., 1981). This uneven distribution of interocular suppression across the visual field of the amblyopic eye could account for reduced suppression of the amblyopic eye in the periphery of the visual field repre-

sentation. However, it does not explain why the amblyopic eye caused stronger BOLD signals than the normal eye.

A further possibility could be attentional modulation, assuming that subjects have to invest more effort when analyzing patterns presented to the amblyopic eye. That attention can enhance BOLD signals also in lower areas including V1 has been documented by Somers, Dale, Seiffert, and Tootell (1999) and Brefczynski and DeYoe (1999). Thus, it is conceivable that increased attentional effort to process signals from the amblyopic eye leads to an increased BOLD signal (Logothetis, Pauls, Augath, Trinath, & Oeltermann, 2001). Several observations seem incompatible with this interpretation. The hypothetical increase of attentional effort did not enhance responses in higher tier visual areas, although they are particularly susceptible to attentional effects (Somers et al., 1999). One possibility is that the amblyopia-related response reduction in higher areas is so pronounced that it cannot be compensated by enhanced attention. This interpretation agrees with the indications for transmission failure from lower to higher visual areas that have been obtained in neurophysiological experiments (Schröder et al., 2002; Sireteanu, 1991; Sireteanu, 2000a, 2000b; Sireteanu & Best, 1992).

4.4. The role of spatial and temporal distortions

In addition to the well-known deficits in visual acuity and contrast sensitivity, strabismic amblyopes frequently experience perceptual distortions, including the perception of spurious contours, spurious movements and spurious colors of high-contrast geometrical patterns (cf. Barrett et al., 2003; Bäumer & Sireteanu, in preparation; Bedell & Flom, 1981, 1983; Bradley & Freeman, 1985; Fronius & Sireteanu, 1989; Hess et al., 1978; Pugh, 1958; Lagrèze & Sireteanu, 1991; Sireteanu et al., 1993; Sireteanu, Bäumer, & Sârbu, 2005). The images perceived through the amblyopic eye appear as constantly moving, as "seen through hot air" (Sireteanu, 2000a).

Several hypotheses have been put forward in order to explain the neural substrate of the perceptual deficits in strabismic amblyopia. Hess et al. (1978) proposed a neural scrambling model ("uncalibrated neural disarray"), in which the normally accurate retinotopic map of the visual world is disturbed in amblyopia. Levi and Klein (1986), Sharma, Levi, and Klein (2000), Sharma, Levi, and Coletta (1999) posited that the amblyopic deficit results from a thinning out of the cortical neurons representing the amblyopic eye ("sparse sampling," or "undersampling"). Sireteanu and colleagues proposed that constant spatial errors in strabismics might be produced by a systematic shift in the neural map, caused by different patterns of retinal correspondence in the central vs. the peripheral visual field; this in turn is related to the different grain of the central vs. peripheral visual field, which leads to a deeper suppression in the central visual field and an anomalous retinal correspondence in the visual periphery (Fronius & Sireteanu, 1989; Lagrèze & Sireteanu, 1991; Sireteanu & Fronius, 1989; Sireteanu, 2000a, 2000b). Barrett et al. (2003) suggested that the non-veridical spatial

perception in amblyopes has its origin in errors in the neural coding of orientation in the primary visual cortex.

Here, we propose an alternative explanation. We suggest that, like other neurodevelopmental disorders, amblyopia might be a two-step process: first, a prenatal predisposition occurs, in form of a still unexplained, congenital, probably genetically determined, weakness of the brain mechanisms responsible for binocular fusion. When children afflicted by this predisposition encounter an otherwise surmountable early ocular problem, like an imbalance of the two eyes due to eye misalignment, anisometropia, a high bilateral ametropia, or a combination of these, a deep suppression of the images of one eye (typically the more affected one) ensues. This leads to a chronic disuse of the central pathway connected to this eye. Cortical cells belonging to this pathway fail to connect to each other and to cells from brain areas subserving other modalities.

Loss of resolution and contrast sensitivity, spatial distortions, crowding and instabilities might be the consequences of this disuse. These consequences affect mainly the ventral pathway, which leads from area 17 to the infero-temporal cortex, but cells on the dorsal pathway, leading to the multisensory association areas in the posterior parietal cortex (Goodale, 1997; Goodale & Milner, 1992; Mishkin & Ungerleider, 1982) and responsible for localizing objects in space and integrating vision with action, might also be affected. This might lead to a loss of precision for localizing visual stimuli, for perceiving visual contours as aligned, for guiding visual attention and preparing for visual action. The unchecked activity of these cells might lead to the reported errors in localization (Simmers, Ledgeway, Hess, & McGraw, 2003), in appreciation of the continuity of contours (Hess et al., 2001) and in eye–hand coordination (Fronius & Sireteanu, 1994). They might also be responsible for the perception of illusory movement in form of temporal instability (Bäumer & Sireteanu, in preparation). Color illusions might also be a consequence of unchecked activity: cortical cells sensitive to colors might be spuriously activated, even in the absence of an objective, adequate stimulus in the outside world (Bäumer & Sireteanu, in preparation).

The perception of spurious contours, spurious movements and spurious colors in some cases of amblyopia might imply that, in these cases, the habitually suppressed pathway becomes, when activated monocularly, *more* active than the routinely used, fellow eye. Like a partially paralyzed limb, activation of the amblyopic eye might require *more* effort and *more* attention and thus might summon *more* resources than those devoted to the fellow eye.

This hypothetical scenario might provide an explanation for the intriguing finding of an *increased* BOLD signal from the amblyopic eye, especially in parts of areas V1 and V2 of some amblyopic subjects: the requirement of the amblyopic pathway on blood oxygenation might be, paradoxically, *higher* than that of the fellow eye. While the increased activation in the primary areas might reflect spurious perceptual events, the *decreased* activation in higher areas on the ventral pathway might reflect the progressive functional disconnection of these areas (Schröder et al., 2002; Sireteanu, 1991, 2000a, 2000b). These suggested mechanisms would affect both strabismic and anisometropic amblyopes and thus explain why we did not observe more marked differences between the two groups.

We still do not know what happens in the visual areas on the dorsal pathway and especially in the motion areas MT and MST of amblyopic subjects; these areas were not investigated in the present study. Psychophysical studies suggest that perception of global motion and translation of vision into movement are affected in amblyopic subjects as well (Fronius & Sireteanu, 1994; Kubová, Kuba, Juran, & Blakemore, 1996; Simmers, Ledgeway, & Hess, 2005; Simmers et al., 2003), implying deficits in the dorsal visual pathway leading to the posterior parietal cortex. Ongoing studies in our laboratory suggest that mapping of auditory onto visual signals is disturbed in amblyopic subjects experiencing anomalous perception, thus suggesting an involvement of higher-order, multisensory areas in the posterior parietal cortex (Sireteanu, 2000a, 2000b; Sireteanu, Bäumer, Sârbu, Tsujimura, & Muckli, in preparation).

If this scenario proves correct, an *increased* activation upon use of the amblyopic eye might be observed in the visual motion areas MT and MST as well, in subjects experiencing temporal distortions. Likewise, an increased activation might be found in color-sensitive areas on the ventral pathway, in subjects experiencing spurious color perception.

4.5. Conclusion

The most consistent result of the present study is the marked reduction of responses to stimulation of the amblyopic eye in higher visual areas of the ventral processing stream both in anisometropic and in strabismic amblyopes. This suggests transmission failure from lower to higher visual areas which is in agreement with data from animal experiments, which show that discharge rates and tuning of individual cells responses to the amblyopic eye are only little if at all affected (Kiorpes et al., 1998; Roelfsema et al., 1994), but provide clear indications for transmission failure towards higher cortical areas (Fries, Schroder, Roelfsema, Singer, & Engel, 2002; Schröder et al., 2002; Sireteanu, 1991; Sireteanu & Best, 1992). One reason for this reduced activation of higher cortical areas could be reduced response synchronization in lower areas (Roelfsema et al., 1994). Reduced synchrony lowers the saliency of neural responses, presumably because it impairs spatial summation in target cells (Usrey & Reid, 1999). Moreover, it is conceivable that impaired temporal correlation of responses in early areas reduces the match between the output activity of lower areas and the receptive field properties of neurons at higher areas. Especially difficult to explain is the enhancement of responses evoked through the amblyopic eye in parts of the lower visual areas. This enhancement exhibited high interindividual variability and may be related to attentional effects

and/or to the notorious heterogeneity of perceptual deficits in amblyopic subjects, which might be due to uncontrollable events in their individual history.

Acknowledgments

References

Algaze, A., Roberts, C., Leguire, L., Schmalbrock, P., & Rogers, G. (2002). Functional Magnetic Resonance Imaging as a tool for investigating amblyopia in the human visual cortes: A pilot study. *Journal of the American Association for Paediatric Ophthalmology and Strabismus, 6*, 300–306.

Amedi, A., Malach, R., Hendler, T., Peled, S., & Zohary, E. (2001). Visuo-haptic object-related activation in the ventral visual pathway. *Nature Neuroscience, 4*, 324–330.

Anderson, S. J., Holliday, I. E., & Harding, G. F. (1999). Assessment of cortical dysfunction in human strabismic amblyopia using magnetoencephalography (MEG). *Vision Research, 39*, 1723–1738.

Barrett, B., Pacey, I., Bradley, A., Thibos, L., & Morill, P. (2003). Nonveridical visual perception in human amblyopia. *Investigative Ophthalmology and Visual Science, 44*(4), 1555–1567.

Barnes, G. R., Hess, R. F., Dumoulin, S. O., Achtman, R. L., & Pike, G. B. (2001). The cortical deficit in humans with strabismic amblyopia. *Journal of Physiology, 533*, 281–297.

Bäumer, C., & Sireteanu, R. (in preparation). Temporal instabilities in amblyopic vision.

Bedell, H., & Flom, M. (1981). Monocular spatial distortion in strabismic amblyopia. *Investigative Ophthalmology and Visual Science, 20*(2), 263–268.

Bedell, H., & Flom, M. (1983). Normal and abnormal space perception. *American Journal of Optometry and Physiological Optics, 60*(6), 426–435.

Bradley, A., & Freeman, R. (1985). Temporal sensitivity in amblyopia: An explanation of conflicting reports. *Vision Research, 25*, 39–46.

Brefczynski, J. A., & DeYoe, E. A. (1999). A physiological correlate of the 'spotlight' of visual attention. *Nature Neuroscience, 2*, 370–374.

Chino, Y. M., Shansky, M. S., Jankowski, W. L., & Banser, F. A. (1983). Effects of rearing kittens with convergent strabismus on development of receptive-field properties in striate cortex neurons. *Journal of Neurophysiology, 50*(1), 265–286.

Demanins, R., & Hess, R. (1996). Effect of exposure duration on spatial uncertainty in normal and amblyopic eyes. *Vision Research, 36*, 1189–1193.

Demer, J. L., Grafton, S., Marg, E., Mazziotta, J. C., & Nuwer, M. (1997). Positron-emission tomographic study of human amblyopia with use of defined visual stimuli. *Journal of the American Association for Paediatric Ophthalmology and Strabismus, 1*, 158–171.

Demer, J. L., von Noorden, G. K., Volkow, N. D., & Gould, K. L. (1988). Imaging of cerebral blood flow and metabolism in amblyopia by positron emission tomography. *American Journal of Ophthalmology, 105*, 337–347.

Duke-Elder, S. (1973). *System of ophthalmology, Vol. VI: Ocular motility and strabismus*. London: Kimpton.

Foster, K. H., Gaska, J. P., Nagler, M., & Pollen, D. A. (1985). Spatial and temporal frequency selectivity of neurones in visual cortical areas V1 and V2 of the macaque monkey. *Journal of Physiology, 365*, 331–363.

Fries, P., Schroder, J. H., Roelfsema, P. R., Singer, W., & Engel, A. K. (2002). Oscillatory neuronal synchronization in primary visual cortex as a correlate of stimulus selection. *Journal of Neuroscience, 22*(9), 3739–3754.

Fronius, M., & Sireteanu, R. (1989). Monocular geometry is selectively distorted in the central field of strabismic amblyopes. *Investigative Ophthalmology and Visual Science, 30*(9), 2034–2044.

Fronius, M., & Sireteanu, R. (1994). Pointing errors in strabismics: Complex patterns of distorted visuomotor coordination. *Vision Research, 34*, 689–707.

Goebel, R., Khorram-Sefat, D., Muckli, L., Hacker, H., & Singer, W. (1998). The constructive nature of vision: Direct evidence from functional magnetic resonance imaging studies of apparent motion and motion imagery. *European Journal of Neuroscience, 10*, 1563–1573.

Goodale, M. A. (1997). Visual routes to perception and action in the cerebral cortex. In F. Boller & J. Grafman (Eds.), *Handbook of neuropsychology, 11* (5), 91–109.

Goodale, M. A., & Milner, D. (1992). Separate visual pathways for perception and action. *Trends in Neuroscience, 15*, 20–25.

Goodyear, B. G., Nicolle, D. A., Humphrey, G. K., & Menon, R. S. (2000). BOLD fMRI response of early visual areas to perceived contrast in human amblyopia. *Journal of Neurophysiology, 84*, 1907–1913.

Goodyear, B. G., Nicolle, D. A., & Menon, R. S. (2002). High resolution fMRI of ocular dominance columns within the visual cortex of human amblyopes. *Strabismus, 10*, 129–136.

Grill-Spector, K. (2001). Semantic versus perceptual priming in fusiform cortex. *Trends in Cognitive Science, 5*, 227–228.

Grill-Spector, K., Kushnir, T., Hendler, T., & Malach, R. (2000). The dynamics of object-selective activation correlate with recognition performance in humans. *Nature Neuroscience, 3*, 837–843.

Hasson, U., Levy, I., Behrmann, M., Hendler, T., & Malach, R. (2002). Eccentricity bias as an organizing principle for human high-order object areas. *Neuron, 34*(3), 479–490.

Hess, R., Campbell, F., & Greenhalgh, T. (1978). On the nature of the neural abnormality in human amblyopia; neural aberrations and neural sensitivity loss. *Pfluegers Archives, 377*, 201–207.

Hess, R. F., Dakin, S. C., & Kapoor, N. (2000). The foveal 'crowding' effect: Physics or physiology? *Vision Research, 40*, 365–370.

Hess, R., Dakin, S., Tewfik, M., & Brown, B. (2001). Contour interaction in amblyopia: Scale selection. *Vision Research, 41*, 2285–2296.

Hess, R., & Howell, E. (1977). The threshold contrast sensitivity function in strabismic amblyopia: Evidence for a two type classification. *Vision Research, 17*, 1049–1055.

Hess, R. F., & Pointer, J. S. (1985). Differences in the neural basis of human amblyopias: The distribution of the anomaly across the visual field. *Vision Research, 25*, 1577–1594.

Hess, R. F., Pointer, J. S., Simmers, A., & Bex, P. (2003). Border distinctness in amblyopia. *Vision Research, 43*, 2255–2264.

Hilz, R., Rentschler, I., & Brettel, H. (1977). Myopic and strabismic amblyopia: Substantial differences in human visual development. *Experimental Brain Research, 30*, 445–446.

Horton, J. C., Hocking, D. R., & Adams, D. L. (1999). Metabolic mapping of suppression scotomas in striate cortex of macaques with experimental strabismus. *Journal of Neuroscience, 19*, 7111–7129.

Imamura, K., Richter, H., Fischer, H., Lennerstrand, G., Franzen, O., Rydberg, A., et al. (1997). Reduced activity in the extrastriate visual cortex of individuals with strabismic amblyopia. *Neuroscience Letters, 225*, 173–176.

Kabasakal, L., Devranoglu, K., Arslan, O., Erdil, T. Y., Sonmezoglu, K., Uslu, I., et al. (1995). Brain SPECT evaluation of the visual cortex in amblyopia. *Journal of Nuclear Medicine, 36*, 1170–1174.

Kieß, S., Sireteanu, R., Goebel, R., Lanfermann, W., & Muckli, L. (2001). Investigating the amblyopic deficit in humans using event-related functional MRI. In H. Bülthoff, K. Gegenfurtner, H. Mallot, & R. Ulrich (Eds.), *Beiträge zur 4. Tübinger Wahrnehmungskonferenz.* Kirchentellinsfurt: Knirsch Verlag.

Kiorpes, L. (2002). Sensory processing: Animal models of amblyopia. In M. Moseley & A. Fielder (Eds.), *Amblyopia: A multidisciplinary approach* (pp. 1–18). Oxford: Butterworth–Heinemann.

Kiorpes, L., Kiper, D. C., O'Keefe, L. P., Cavanaugh, J. R., & Movshon, J. A. (1998). Neuronal correlates of amblyopia in the visual cortex of macaque monkeys with experimental strabismus and anisometropia. *Journal of Neuroscience, 18*, 6411–6424.

Kiorpes, L., & McKee, S. P. (1999). Neural mechanisms underlying amblyopia. *Current Opinion in Neurobiology, 9*, 480–486.

Kriegeskorte, N., & Goebel, R. (2001). An efficient algorithm for topologically correct segmentation of the cortical sheet in anatomical MR volumes. *NeuroImage, 14*, 329–346.

Kubová, Z., Kuba, M., Juran, J., & Blakemore, C. (1996). Is the motion system relatively spared in amblyopia? Evidence from cortical evoked responses. *Vision Research, 36*, 181–190.

Lagrèze, W.-D., & Sireteanu, R. (1991). Two-dimensional spatial distortions in human strabismic amblyopia. *Vision Research, 31*, 1271–1288.

Lee, K. M., Lee, S. H., Kim, N. Y., Kim, C. Y., Sohn, J. W., Choi, M. Y., et al. (2001). Binocularity and spatial frequency dependence of calcarine activation in two types of amblyopia. *Neuroscience Research, 40*, 147–153.

Leonards, U., & Sireteanu, R. (1993). Interocular suppression in normal and amblyopic subjects: The effect of unilateral attenuation with neutral density filters. *Perception and Psychophysics, 54*, 65–74.

Lerner, Y., Pianka, P., Azmon, B., Leiba, H., Stolovitch, C., Loewenstein, A., et al. (2003). Area-specific amblyopic effects in human occipitotemporal object representations. *Neuron, 40*, 1023–1029.

Levi, D. M., & Klein, S. (1983). Spatial localization in normal and amblyopic vision. *Vision Research, 23*, 1005–1017.

Levi, D. M., & Klein, S. A. (1985). Vernier acuity, crowding and amblyopia. *Vision Research, 25*, 979–991.

Levi, D. M., & Klein, S. A. (1986). Sampling in spatial vision. *Nature, 320*, 360–362.

Levy, I., Hasson, U., Avidan, G., Hendler, T., & Malach, R. (2001). Center-periphery organization of human object areas. *Nature Neuroscience, 4*, 533–539.

Linden, D. E., Kallenbach, U., Heinecke, A., Singer, W., & Goebel, R. (1999). The myth of upright vision. A psychophysical and functional imaging study of adaptation to inverting Spectacles. *Perception, 28*(4), 469–481.

Logothetis, N. K., Pauls, J., Augath, M., Trinath, T., & Oeltermann, A. (2001). Neurophysiological investigation of the basis of the fMRI signal. *Nature, 412*, 150–157.

Malach, R., Reppas, J. B., Benson, R. R., Kwong, K. K., Jiang, H., Kennedy, W. A., et al. (1995). Object-related activity revealed by functional magnetic resonance imaging in human occipital cortex. *Proceedings of the National Academy of Science USA, 92*, 8135–8139.

Mishkin, M., & Ungerleider, L. (1982). Contribution of striate inputs of the visuospatial functions of parieto-preoccipital cortex in monkeys. *Behavioral Brain Research, 6*, 57–77.

Muckli, L., Tonhausen, N., Goebel, R., Lanfermann, H., Zanella, F. E., Singer, W., et al. (1998). Reduced fMRI response to monocular amblyopic eye stimulation in extrastriate visual areas. *NeuroImage, 7*(4), 19.

Muckli, L., Kohler, A., Kriegeskorte, N., & Singer, W. (2005). Primary visual cortex activity along the apparent-motion trace reflects illusory perception. *PLoS Biology, 3*(8), e265.

Pugh, M. (1958). Visual distortion in amblyopia. *British Journal of Ophthalmology, 42*, 449–460.

Ress, D., Backus, B. T., & Heeger, D. J. (2000). Activity in primary visual cortex predicts performance in a visual detection task. *Nature Neuroscience, 3*(9), 940–945.

Ress, D., & Heeger, D. J. (2003). Neuronal correlates of perception in early visual cortex. *Nature Neuroscience, 6*(4), 414–420.

Roelfsema, P. R., König, P., Engel, A. K., Sireteanu, R., & Singer, W. (1994). Reduced synchronization in the visual cortex of cats with strabismic amblyopia. *European Journal of Neuroscience, 6*, 1645–1655.

Schröder, J. H., Fries, P., Roelfsema, P. R., Singer, W., & Engel, A. K. (2002). Ocular dominance in extrastriate cortex of strabismic amblyopic cats. *Vision Research, 42*, 29–39.

Sereno, M. I., Dale, A. M., Reppas, J. B., Kwong, K. K., Belliveau, J. W., Brady, T. J., et al. (1995). Borders of multiple visual areas in humans revealed by functional magnetic resonance imaging. *Science, 268*, 889–893.

Sharma, V., Levi, D., & Klein, S. (2000). Undercounting features and missing features: Evidence for a high-level deficit in strabismic amblyopia. *Nature Neuroscience, 3*(5), 496–501.

Sharma, V., Levi, D. M., & Coletta, N. J. (1999). Sparse sampling of gratings in the visual cortex of strabismic amblyopes. *Vision Research, 39*, 3526–3536.

Simmers, A., Ledgeway, T., & Hess, R. (2005). The influences of visibility and anomalous integration processes on the perception of global spatial form versus motion in human amblyopia. *Vision Research, 45*, 449–460.

Simmers, A., Ledgeway, T., Hess, R., & McGraw, P. (2003). Deficits to global motion processing in human amblyopia. *Vision Research, 43*, 729–738.

Singer, W., von Grünau, M., & Rauschecker, J. (1980). Functional amblyopia in kittens with unilateral exotropia. I. Electrophysiological assessment. *Experimental Brain Research, 40*, 294–304.

Singh, K. D., Smith, A. T., & Greenlee, M. W. (2000). Spatiotemporal frequency and direction sensitivities of human visual areas measured using fMRI. *NeuroImage, 12*, 550–564.

Sireteanu, R. (1982). Human amblyopia: Consequence of chronic interocular suppression. *Human Neurobiology, 1*, 31–33.

Sireteanu, R. (1991). Restricted visual fields in both eyes of kittens raised with a unilateral, surgically induced strabismus: Relationship to extrastriate cortical binocularity. *Clinical Vision Sciences, 6*(4), 277–287.

Sireteanu, R. (2000a). The binocular visual system in amblyopia. *Strabismus, 8*, 39–51.

Sireteanu, R. (2000b). The binocular act in strabismus. In G. Lennerstrand & J. Ygge (Eds.), *Advances in strabismus research: Basic and clinical aspects* (pp. 63–83). London, UK: Portland Press.

Sireteanu, R., Bäumer, C., & Sârbu, C. (2005). Temporal instability of amblyopic vision: Evidence for an involvement of the dorsal visual pathway. *Journal of Vision, 81*.

Sireteanu, R., Bäumer, C., Sârbu, C., Tsujimura, S., & Muckli, L. (in preparation). Verzerrte Raumwahrnehmung und zeitliche Instabilität bei Schielamblyopie: Psychophysik und Bildgebende Verfahren. *Klinische Monatsblätter der Augenheilkunde.*

Sireteanu, R., & Best, J. (1992). Squint-induced modification of visual receotive fields in the lateral suprasylvian cortex of the cat: Binocular interaction, vertical effect and anomalous correspondence. *European Journal of Neuroscience, 4*, 235–242.

Sireteanu, R., & Fronius, M. (1981). Naso-temporal asymetries in human amblyopia: Consequence of long-term interocular suppression. *Vision Research, 21*, 1055–1061.

Sireteanu, R., & Fronius, M. (1989). Different patterns of retinal correspondence in the central and peripheral visual field of strabismics. *Investigative Ophthalmology and Visual Sciences, 30*, 1023–1033.

Sireteanu, R., Fronius, M., & Singer, W. (1981). Binocular interaction in the peripheral visual field of humans with strabismic and anisometropic amblyopia. *Vision Research, 21*, 1065–1074.

Sireteanu, R., Lagrèze, W.-D., & Constantinescu, D. H. (1993). Distortions in two-dimensional visual space perception in strabismic observers. *Vision Research, 33*, 677–690.

Sireteanu, R., & Singer, W. (1980). The "vertical effect" in human squint amblyopia. *Experimental Brain Research, 40*, 354–357.

Sireteanu, R., Tonhausen, N., Muckli, L., Lanfermann, H., Zanella, F. E., Singer, W., et al. (1998). Cortical site of the amblyopic deficit in strabismic and anisometropic subjects, investigated with fMRI. *Investigative Ophthalmology and Visual Sciences, 39*, 909.

Somers, D. C., Dale, A. M., Seiffert, A. E., & Tootell, R. B. (1999). Functional MRI reveals spatially specific attentional modulation in human

primary visual cortex. *Proceedings of the National Academy of Sciences USA, 96*, 1663–1668.

Thiele, A., Bremmer, F., Ilg, U. J., & Hoffmann, K. P. (1997). Visual responses of neurons from areas V1 and MT in a monkey with late onset strabismus: a case study. *Vision Research, 37*, 853–863.

Tootell, R. B., & Hadjikhani, N. (2001). Where is 'dorsal v4' in human visual cortex. retinotopic, topographic and functional evidence. *Cerebral Cortex, 11*, 298–311.

Tootell, R. B., Mendola, J. D., Hadjikhani, N. K., Ledden, P. J., Liu, A. K., Reppas, J. B., et al. (1997). Functional analysis of V3A and related areas in human visual cortex. *Journal of Neuroscience, 17*, 7060–7078.

Tootell, R. B. H., Hadjikhani, N. K., Mendola, J. D., Marrett, S., & Dale, A. M. (1998). From retinotopy to recognition: fMRI in human visual cortex. *Trends in Cognitive Science, 2*, 174–183.

Usrey, W. M., & Reid, R. C. (1999). Synchronous activity in the visual system. *Annual Reviews of Physiology, 61*, 435–456.

von Noorden, G. K. (1980). *Burian–von Noorden's binocular vision and ocular motility*. St. Louis, MO: Mosby.

Wang, H., Levi, D., & Klein, S. (1998). Spatial uncertainty and sampling efficiency in amblyopic position acuity. *Vision Research, 38*, 1239–1251.

Wiesel, T. N. (1982). Postnatal development of the visual cortex and the influence of environment. *Nature (London), 299*, 582–591.

Wiesel, T. N., & Hubel, D. H. (1963). Single-cell responses in striate cortex of kittens deprived of vision in one eye. *Journal of Neurophysiology, 26*, 1003–1017.

Yu, C., & Levi, D. M. (1998). Naso-temporal asymmetry of spatial interactions in strabismic amblyopia. *Optometry and Visual Science, 75*, 424–432.